Impacts of environmentally relevant levels of the perfluorooctanoic acid (PFOA) replacement compound GenX (Hexafluoropropylene Oxide Dimer Acid) on feeding behavior, mitochondrial ROS, and gene expression in *Caenorhabditis elegans*

By

Monica Storm Cash

Director of Thesis: Xiaoping Pan, PhD

July 2023

Major Department: Department of Biology

Per- and polyfluoroalkyl substances (PFAS) are commercially manufactured chemicals known for widespread usage in different industries. Past research indicating negative health impacts and bioaccumulation in humans and the environment have resulted in the withdrawal and banning of some PFAS. GenX is a short-chained replacement for a long-chained PFAS, but an insufficient amount of research has been conducted on the potential health impacts of GenX to justify its growing prominence and its increasing exposures to humans and the environment, such as commercial dumping into residential waterways. GenX levels correlating to the concentrations found in the Cape Fear River were evaluated using *Caenorhabditis elegans* as a model organism to measure a neurological toxicity behavior, reactive oxygen species accumulation, and select genetic regulation changes. Neurological toxicity behavior in the form of pharyngeal pumping was used to determine if the excitatory effects of legacy PFAS apply to GenX and were found to have significantly substantive evidence. Potential symptoms mitochondrial toxicity in the form of semi-quantitative recordings of reactive oxygen species and

genetic analysis of genes of interest were assessed as well with areas of further investigation identified.

Impacts of environmentally relevant levels of the perfluorooctanoic acid (PFOA) replacement compound GenX (Hexafluoropropylene Oxide Dimer Acid) on feeding behavior, mitochondrial ROS, and gene expression in *Caenorhabditis elegans*

A Thesis

Presented To

The Faculty of the Department of Biology

East Carolina University

In Partial Fulfilment of the Requirements for the Degree

Master of Science in Biology

By:

Monica Storm Cash

Director of Thesis: Xiaoping Pan, PhD

Impacts of environmentally relevant levels of the perfluorooctanoic acid (PFOA) replacement compound GenX (Hexafluoropropylene Oxide Dimer Acid) on feeding behavior, mitochondrial ROS, and gene expression in *Caenorhabditis elegans*

By:

Monica Storm Cash

APPROVED BY:

DIRECTOR OF THESIS:

_____

Xiaoping Pan, PhD

COMMITTEE MEMBER:

_____

Baohong Zhang, PhD

COMMITTEE MEMBER:

_____

David Collier, MD, PhD, FAAP

COMMITTEE MEMBER:

_____

Kimberlee Caldwell, PhD

CHAIR OF THE DEPARTMENT OF BIOLOGY:

_____

David Chalcraft PhD

DEAN OF THE GRADUATE SCHOOL:

_____

Kathleen Cox, PhD

Acknowledgements

I would like to thank my committee advisors for serving on my defense committee and ensuring the quality of my work through their expertise. I would like to thank my thesis advisor, Dr. Xiaoping Pan, for her mentorship and support throughout my studies at East Carolina University. I would like to thank the professors and staff members who mentored me when I did not know how to ask—Dr. Patrick Horne for his compassion as my Biochemistry professor and Dr. Fadi Issa for his training and trust in proper equipment usage of the LSM 800 confocal microscope and interest in my thesis.

Thank you, ECU Biology Department for funding travel to conferences where I learned the invaluable lesson of the importance of my research, and thank you to the residents who attended the 3rd Annual PFAS Conference and spoke about their experiences being impacted by PFAS.

I would like to thank my parents for their love and warmth towards me as I have progressed through my education, especially for my mother who ensured I had a "nest" to return home to when breaks were needed.

And lastly, I cannot express enough gratitude to my friends— J. Hugh Wright III, Grey Hutchinson, and Syd Holt— who together more than anyone else, asked about how my research was going and listened, who marveled at the images that I texted them and kept me company on late nights of synchronizing worms when I otherwise would be alone, and who provided the movie nights at the end of the weekday that kept me sane. They were there through all the high and low points of my thesis research, especially Hugh whom I knew I could always call. I am glad that I can acknowledge all three of your impacts on this thesis.

Table of Contents

List of Tables

List of Figures

Introduction

Per- and polyfluoroalkyl substances (PFAS) are commercially used chemicals known for their resistance to degradation and widespread usage in various industries (Brase et al. 2021). Past and ongoing environmental pollution from widespread commercial manufacturing and continued utilization have caused measurable levels of PFAS in humans due to occupational hazards, drinking water, and dietary intake (Brase et al. 2021). Past research has indicated the potential toxicological effects of PFAS accumulation in humans and the environment (Foguth et al. 2020), resulting in some long-chained PFAS becoming banned while others were voluntarily replaced by the primary manufacturer in 2001 (US EPA 2000; Foguth et al. 2020). As substances that do not fully degrade and have the capacity to bioaccumulate (Brase et al. 2021), the lack of complete understanding on the effects of PFAS on human health is a concern (Foguth et al. 2020). Short-chained PFAS have replaced some long-chained PFAS in the justification that short-chains will not bioaccumulate in animal tissues and the environment to the same extent as long-chains (Brendel et al. 2018; Jabeen et al. 2020). However, many gaps in research exist to determine if the idea is supported (Foguth et al. 2020; Gaballah et al. 2020). Examples of short-chain PFAS with long half-lives are notable inconsistencies to the conclusion (Foguth et al. 2020), and comparative animal studies and human studies on the potential health impacts of short-chained PFAS are lacking (Foguth et al. 2020).

One of the short-chained molecules to replace long-chained perfluorooctanoic acid (PFOA), a type of PFAS, is GenX, the trade name for the ammonium salt of hexafluoropropylene oxide–dimer acid (HFPO-DA) (Hopkins et al. 2018). The chemical is also known as 2,3,3,3-tetrafluoro-2-(heptafluoropropoxy)propanoic acid, FRD-903, and undeca- or perfluoro-2-methyl-3-oxahexanoic acid (Houck et al. 2021). Beneath the umbrella classifications

of PFAS, GenX classified as a perfluoroalkyl ether carboxylic acid (PFECA) in which a carboxyl group has replaced a fluorine in PFOA (Figure 1).

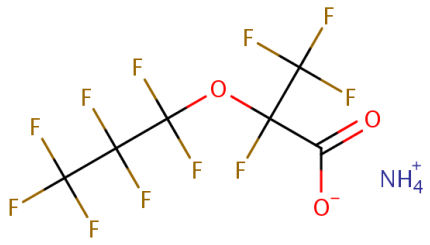

Figure 1. GenX chemical structure in ammonium salt form (DTXSID40108559) (CompTox)

In 2015, GenX was identified in the Cape Fear River off the coast of North Carolina at rates above the health advisory level in nearly half of all days surveyed in the study (Strynar et al. 2015). GenX was later detected in residential water within the Cape Fear River Basin, downstream of the responsible manufacturing plant (Hopkins et al. 2018). The influx into residential water is especially concerning since GenX is not removable in wastewater treatment plants by conventional means (Hopkins et al. 2018). In 2017, raw drinking water from the Cape Fear River in North Carolina was found to have an average GenX concentration of 631 ng/L, four times greater than the then-estimated safe level of 140 ng/L (Gaballah et al. 2020). Peak area counts of the "emerging PFASs," in this case a mix comprised primarily of two different three-carbon PFASs (PFMOAA and PFO2HxA), were as high as 160,000 ng/L in finished drinking water drawn from the Cape Fear River (Hopkins et al. 2018) from chemical degradation from the parent PFAS compounds into derivative forms. Additionally, the half-life of hexafluoropropylene oxide dimer acid (HFPO-DA), the GenX species found in the Cape Fear River Basin, is not yet known in humans (Jabeen et al. 2020). Outside of North Carolina, GenX

has been detected in environmental samples in Ohio and West Virginia of the United States, Germany, China, the Netherlands, England, South Korea, and Sweden (Conley et al. 2021). The wide range from manufacturing sites to detection sites indicates that local environmental exposures are not isolated events. GenX may have the similar potential to become transported further than the source location and accumulate in organisms and the environment as long-chained-PFAS have done (Greaves and Letcher 2013). Despite humans and the environment increasingly becoming exposed to GenX, little information is known regarding its expected impact on human health and the environment outside of commercial claims.

As a newly developed chemical, literature on GenX has yet to fully develop. However, early animal model studies indicate similar health effects as PFAS (e.g. Foguth et al. 2020). Animal models are frequently used to provide a deeper understanding of how a toxicant may impact humans (Foguth et al. 2020). By referencing animal models in studies on exposure, a greater understanding of the potential human impact can be developed. From the early research conducted, GenX has been shown to be a potential developmental toxicant (Thompson et al. 2019; Conley et al. 2021), with negative impacts on pregnancies similar to legacy PFAS in rats and mice (Blake et al. 2020; Conley et al. 2021). GenX has also been found to disrupt metabolism and other necessary biochemical pathways, specifically the PPAR signaling pathways (Conley et al. 2021; Houck et al. 2021), with a decrease in the transport activity of p-glycoprotein and breast cancer resistance protein in rat models (Cannon et al. 2020). In addition to protein signaling pathways, GenX was found to significantly upregulate protein coding genes associated with mitochondrial energy pathways (*Cpt1b, Cpt2, Acadl, Acadm, Acaa2*) and increase the accumulation of reactive oxygen species (*Txnip*) in rats (Conley et al. 2021). While closer species surrogates are needed to fully support the transference of predicted toxicological

effects from animals to humans (Corton et al. 2014), lower order species provide insight into areas worth investigating (Foguth et al. 2020).

This research paper investigated the effects of GenX exposure on pharyngeal pumping behaviors, reactive oxygen species (ROS) accumulation in the pharynx, and the selected genetic regulation after set time exposures to GenX in *Caenorhabditis elegans*. *C. elegans* are a common model organism in toxicology studies due to their low maintenance, short life cycles, and fully sequenced DNA (Caldwell et al. 2018; Foguth et al. 2020). The *C. elegans* pharynx consists of three anatomic units: the corpus, isthmus, and terminal bulb (Figure 2). The pump draws the bacterial food into the corpus at the anterior end. The food is transferred along the isthmus and then crushed by the V-shaped grinder located in the terminal bulb before passing into the intestine for absorption (Hall and Altum 2008). Pharyngeal muscles consist of twenty cells of eight different divisions and serve to open the lumen for pharyngeal pumping and feeding. The body-wall muscles of *C. elegans* contain abundant mitochondria (Kim et al. 2018) as an active structure responsible for food consumption. The muscle belly and muscle arm to the nerve ring were the regions of the assessed reactive oxygen species due to the role of the pharyngeal pump in *C. elegans*.

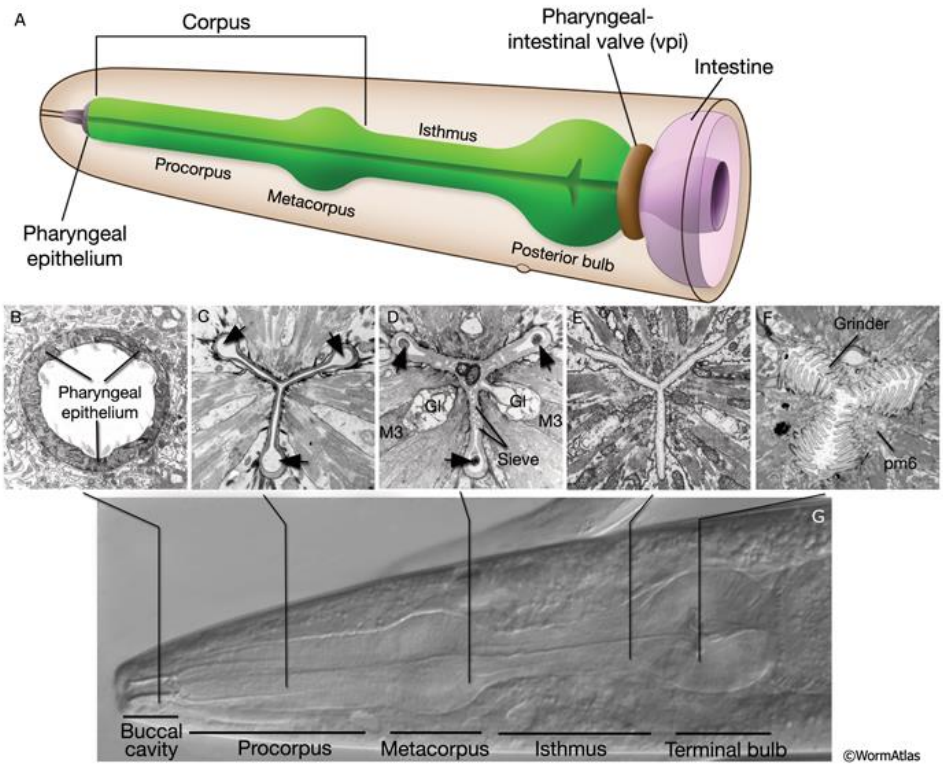

Figure 2. *C. elegans* Pharynx Diagram (WormAtlas)

Several comparisons suggest an evolutionary relationship between the *C. elegans* pharynx and the vertebrate heart to support the *C. elegans* pharynx serving as an animal model to the vertebrate heart. Three genes are shared between *C. elegans* and vertebrates as a part of an evolutionary conserved mechanism responsible for pharyngeal development and the vertebrate heart, respectively (Chen and Fishman 1996; Huan et al. 1998; Mango 2007). In development, both organs rely on NKX transcription factors for their formation (Chen and Fishman 1996; Okkema et al. 1997). Both the pharynx and the heart have similar electrical circuitry to control pumping with both using T- and L-type Ca^{2+} channels for its action potential (Chen and Fishman 1996; Bernstein and Morley 2006). Both structures' contractions are synchronized junctions that couple adjacent muscle cells, and contractions can continue in the absence of neuronal input (Avery and Horvitz 1989; Bernstein and Morley 2006) with the pumping speed modulated by

neurotransmitters such as acetylcholine and serotonin (Hobson et al. 2003). For these reasons, data about the effects on the pharyngeal pumping of *C. elegans* can provide insights into the potential effects on the vertebrate heart.

Mitochondrial toxicity is a method of measuring the impact of a pollutant on mitochondria, the cellular organelle primarily responsible for energy production and oxygen consumption within an organism (Zheng et al. 2021). Though reactive oxygen species (ROS) are essential in many physiological biochemical pathways (Dröge 2002) such as immune system function and basic development processes (Meyers et al. 2018), malformed mitochondria overproduce reactive oxygen species and cause cellular damage and diseases (Zheng et al. 2021) such as neurodegeneration from the imbalance of fission and fusion that leads to an accumulation of structural defects and cell death (Kim et al. 2018). An estimated 1 in 4,300 people are reported to have a mitochondrial disease (Gorman et al. 2015) that would place them at greater risk of exacerbating diseases from toxicant exposure (Meyers et al. 2018). Additionally, damage from mitochondrial toxicity has been reported to pass onto further generations due to genetic inheritance (Meyers et al. 2018). Little research has been conducted on mitochondrial gene-environment interactions (Meyers et al. 2018), but gene expression studies are available to study the impact of toxicants on mitochondria (Zheng et al. 2021). With mitochondria key in multiple biochemical pathways, phenotypic damage and ROS over- or underproduction causes potential disfunction within the organelle and potentially the cell and organism, depending on the extent.

Since GenX has been the focus of few studies, comparisons to PFAS neurotoxicity studies provide information on starting points to potential GenX neurotoxic effects. Similar to the findings that PFOS increases hyperactivity in *C. elegans*, PFOS caused dopaminergic neurotoxicity and neurotoxicity in γ-aminobutyric acid (GABA)ergic, serotonergic, and

cholinergic neurons in dosed *Caenorhabditis elegans* and decreased mitochondria count (Sammi et al. 2019), which indicates the potential for mitochondrial morphology defects and/or genetic regulation related to mitochondrial toxicity. Genes of interest related to pharyngeal pumping and mitochondrial fission and fusion have been selected (Table 1) to determine if GenX causes any potential effects.

Table 1. Genes of Interest. The table lists protein-coding genes of interest used in assessing mitochondrial toxicity due to role in pharyngeal pumping and/or mitochondrial health. A brief description of functions is provided by WormBase.

Gene	Description
Drp-1	Predicted to enable GTP binding activity; GTPase activity; and microtubule binding activity. Involved in apoptotic mitochondrial changes; embryo development; and mitochondrial fission. Located in mitochondrion. Expressed in several structures, including germ line; non-striated muscle; preanal ganglion; rectal muscle; and somatic nervous system. Human ortholog(s) of this gene implicated in Alzheimer's disease; encephalopathy due to defective mitochondrial and peroxisomal fission 1; optic atrophy 5; and pulmonary fibrosis. Is an ortholog of human DNM1L (dynamin 1 like).
Eat-2	Enables acetylcholine-gated cation-selective channel activity. Involved in several processes, including feeding behavior; positive regulation of multicellular organismal process; and regulation of eating behavior. Located in neuromuscular junction and plasma membrane. Part of acetylcholine-gated channel complex. Expressed in pm4 and pm5. Human ortholog(s) of this gene implicated in several diseases, including Alzheimer's disease; Lewy body dementia; carcinoma (multiple); and inflammatory bowel disease (multiple). Is an ortholog of human CHRFAM7A (CHRNA7 (exons 5-10) and FAM7A (exons A-E) fusion) and CHRNA7 (cholinergic receptor nicotinic alpha 7 subunit).
Eat-18	Involved in chemical synaptic transmission and regulation of pharyngeal pumping. Predicted to be located in membrane.
Egl-19	Enables voltage-gated calcium channel activity. Involved in several processes, including determination of left/right asymmetry in nervous system; positive regulation of striated muscle contraction; and regulation of pharyngeal pumping. Located in plasma membrane. Expressed in several structures, including alimentary muscle; body wall musculature; neurons; preanal ganglion; and tail. Used to study Duchenne muscular dystrophy. Human ortholog(s) of this gene implicated in several diseases, including Brugada syndrome 3; Timothy syndrome; and X-linked recessive disease (multiple). Is an ortholog of human CACNA1C (calcium voltage-gated channel subunit alpha1 C); CACNA1F (calcium voltage-gated channel subunit alpha1 F); and CACNA1S (calcium voltage-gated channel subunit alpha1 S).

Spe-6	Predicted to enable protein serine/threonine kinase activity. Involved in male meiosis chromosome separation; regulation of protein localization; and spermatid differentiation. Predicted to be located in nucleus. Expressed in sperm.

Hypothesis

1. Pharyngeal pumping will significantly increase from GenX exposure.

2. Mitochondrial ROS production will significantly increase from GenX exposure.

3. Gene expression will significantly alter following GenX exposure.

Objectives

1. Determine impact of GenX on the pharyngeal pumping behavior in *C. elegans*
2. Compare mitochondrial ROS levels in control and GenX treated worms
3. Investigate the selected gene expressions following GenX exposure

Methods

Pharyngeal Pumping

Bristol N2 wild-type worms were synchronized and collected at the L4 stage. They were then exposed to GenX at 0, 14, 140, 700, 1400, 7000, 14,000, and 71,000 ng/L in K-medium (0.0032M KCl and 0.051M NaCl) through liquid exposure with OP50 added to prevent starvation conditions. The first seven concentrations correspond to 0x, 0.1x, 1x, 5x, 10x, 50x, and 100x, respectively, of the previous North Carolina Department of Health and Human Services' estimated safe drinking water equivalent level (DWEL) of 140 ng/L of GenX (The DWEL calculated for bottle-fed infants based on the reference dose of 0.0001mg/kg/day). The 700 ng/L level approximately corresponds with the average level of 631 ng/L measured in the unprocessed drinking water of the Cape Fear River (Hopkins et al. 2018), and the 71,000 ng/L level corresponds to NC DHHS's prior DWEL based on the European Chemistry Agency's derived no effect level (DNEL) of 0.01 mg/kg/day (NC DHHS, 2017). The experimental dosages for pharyngeal pumping were verified via liquid chromatography-tandem mass spectrometry by an analytical team at North Carolina State University.

After toxicant exposure, the worms were washed with M9 buffer (3 g KH_2PO_4, 6 g Na_2HPO_4, 5 g NaCl, 1 ml 1 M $MgSO_4$, 1 L H_2O) four times to remove remnants of the toxicant and OP50. Then the worms were set on a microscope slide of 2% agarose live to record movements. Videos were taken at 24, 48, and 72 hours post-treatment in thirty second intervals using a light compound microscope at 40x magnification and a LasEZ software to record pharyngeal pump behavior. The terminal bulb was used to count the number of pumps due to the evolutionary relation to the vertebrate heart and function as responsible for food passing into the intestines. The iMovie software was used to slow down the original video to half of its original speed for accurate counting for the pharyngeal pumping. The averages of the thirty seconds were

then doubled to correspond to pumps/min. as the timescale unit. Each worm video was counted three times and then averaged for the normalized count data for analysis. The pharyngeal pumps in response to GenX exposure were analyzed using SPSS to determine significant changes.

Calculating GenX Dosages for Exposure for Mitochondrial ROS and Genetic Analysis

The GenX dosages used for the mitochondrial ROS and genetic analysis were created through the following: The molecular weight of the 97% undecafluoro-2-methyl-3-oxahexanoic acid (Matrix Scientific (Columbia, SC); CAS [13252-13-6]) is 330.06 g/mol in liquid suspension. Specific gravity found 1 uL of the solution to weigh 0.0023g. Creating dosage treatments involved serial dilution from one 25 mL Falcon centrifuge tube to subsequent tubes to achieve 14 ng/L, 140 ng/L, and 700 ng/L using K-medium as working solution.

A modified version of the Zheng et al. (2021) procedure (Appendix C) was used to adjust for the needs of the experimental procedure. Zheng et al. (2021) procedure instructed exposure to the 0.2 mL 5 mM MitoSOX mitochondrial superoxide indicator dye and toxicant on a NGM agar plate. Zheng et al. (2021) altered the manufacture instructions of MitoSOX Red from the advertised live cells to apply to live *C. elegans* using a higher concentration. MitoSOX working stock produces 13 uL liquid, and ten tubes are included per ordered package. In early assessment of experimental design, it was determined that a high volume of MitoSOX Red (ThermoFisher; USA) would have been needed if the dye was to be incorporated into the NGM agar plate. The typical size of NGM agar plates used are 15-17 mL of agar, but the size of 3 mL plate was an option as well for exposure. Based on calculations, the lowest NGM agar exposure would have required approximately one package tube per 25 exposure plates for the recommended 0.2 mL 5 mM MitoSOX dye:

15 mL NGM agar plate: $\frac{0.2\ mL\ MitoSOX}{100\ mL\ agar} = \frac{0.03\ mL\ MitoSOX}{15\ mL\ agar}$, or 30 uL MitoSOX stock solution per plate at the maximum

3 mL NGM agar plate: $\frac{0.2\ mL\ MitoSOX}{100\ mL\ agar} = \frac{0.006\ mL\ MitoSOX}{3\ mL\ agar}$, or 0.6 uL MitoSOX stock solution x 25 3mL plates = 15 uL working stock required for 25 plates at the minimum

While using 3 mL NGM plates may have been feasible, the required concentration would have limited the number of runs in procedure and replicates used. Additionally, the higher concentration of GenX used would have introduced a higher volume of GenX into the local biohazardous waste management for 24 hour usage. Liquid exposure to the dye through a 2 mL tubule for the 24 hours exposure period in a 20°C incubator produced good quality staining underneath the confocal microscope in preliminary trials. The liquid exposure method to the dye and toxicant was decided as the method to proceed.

Mitochondrial Reactive Oxygen Species

The Bristol N2 wild-type strain was synchronized following the Pan lab procedure (Appendix A). After 40-44 hours of growth after synchronization on a NGM plate seeded with 0.25 mL of OP50 in a 20°C incubator, the worms were young adults in L3 stage. The worms were washed with M9 four times in a 2 mL tube with a centrifuge to separate worms from liquid and prevent loss of worms.

For the control group, 2 uL working solution of MitoSOX Red, 1 mL of M9, and 10 uL of OP50 were applied to the washed *C. elegans* within the 2 mL tube for the dye exposure of 24 hours. For the treatment groups, the 14, 140, and 700 ng/L of GenX dosage, respectively by assigned treatment group, was additionally added during the stage for toxicant and dye exposure simultaneously.

After exposure, the tube was centrifuged and washed with M9 four times to remove the external dye. The *C. elegans* were then added to a NGM plate with 0.5 mL of OP50 to rest for an

hour and allow the remanent of MitoSOX Red to clear from the gut. After an hour, the *C. elegans* were washed with M9 three times before being placed via a 15 uL droplet onto a microscope slide with 4% agarose pad and 10 uL of 10 mM levamisole (Figure 3). Using a worm pick as advised by Zheng et al. (2021) procedure was attempted in early testing but determined to be a constraint. While not using the pick did not allow the precise choice of worms, collecting worms through using the pipette allowed for a greater concentration of worms to choose adults for imaging from the microscope slide.

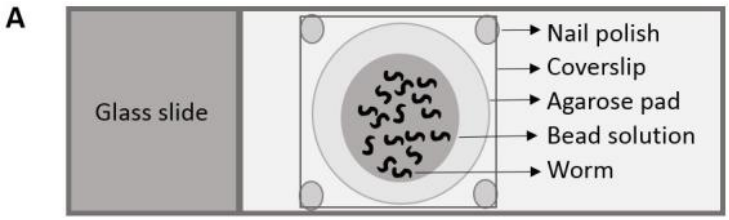

Figure 3. Illustration of *C. elegans* in vivo positioning on microscope slide (Sarasija and Norman 2018)

The worms were imaged using a Zeiss LSM 800 Confocal microscope, often within an hour but at maximum four hours, after producing the microscope slides. The time constraint between slide making and imaging is due to the importance of scanning the worms while they are alive. The MitoSOX Red binds to a reactive oxygen species while the worms are alive. In preliminary attempts, the image quality was found to be poor within 24 hours, likely as the worms began to die. Additionally, levamisole may affect mitochondria after a period of time (Smith et al. 2015). Imaging soon after plating the worms was made a priority in collecting images, and no images were collected after four hours had elapsed.

Settings for the microscope and adjustments for image quality and retention of pixels were calibrated for each worm before imaging to ensure effectiveness for later analysis. The imaging underneath the confocal microscope focused on the pharyngeal bulb up to the

pharyngeal-intestinal valve (Figure 2) at 40x oil. The resulting images were stored in the original file format by the Zeiss LSM 800 Confocal microscope as CZI files and will be stored on a USB thumb drive in the Pan lab for future referencing.

ImageJ is a Java-based, open-source software analysis tool for images with the capacity to measure fluorescence within images. Following Bankhead (2014)'s guidelines, the files were converted from CZI files to TIFF files to prevent the compression and loss of pixel data that may result from other file conversions such as from CZI to JPEG. The confocal microscope was used to convert the individual files from each z-stack into a folder which were stored on the thumb drive. Worth noting to the analysis quality is the process of conversion from CZI to TIFF displays the images as grayscale while keeping the red, blue, and green color system data intact.

As a fluorescent image, the data collected from the samples is based on pixels within the image representing the light emitted by the sample (Bankhead 2014; e.g. Figure 7). For analyzing z-stack images, sum projections (in which all of the pixels located in an *xy* space are summed together into one image) and maximum intensity projections (in which images are compared and only the largest *xy* pixels are displayed) were options for handing stacks after consolidation into one stacked image. Maximum intensity projections was chosen to eliminate the potential impact of using a different number of slices per stacked image (Bankhead 2014). All of the images were used in the creation of a stack for a complete image of the worm rather than selecting to filter certain images. Removing background influence in the images' region of interest was done by ImageJ's program with the rolling ball radius set at 100 pixels as the threshold, following the Bankhead (2014) description for determining rolling ball threshold (Appendix E). The data was measured by ImageJ in the units of mean fluorescence intensity (mfi).

Gene Assessment

Bristol N2 wild-type worms were used in genetic analysis procedures to assess potential impact of GenX on mitochondrial toxicity and pharyngeal pumping genes. *C. elegans* were grown on NGM plates seeded with OP50 until the majority were at L4 stage though different stages were not excluded to provide variety to age. The worms were washed in M9 four times to remove remnants of OP50 and then exposed to respective concentration of GenX in K-medium in a 21°C incubator for 24 hours. After 24 hours, the worms were washed four times in M9 to remove remnants of exterior GenX and OP50. The worms were allowed to rest on a NGM plate seeded with 0.25 mL of OP50 for an hour to recover from stress conditions. After an hour, the worms were washed four times to remove remnants of OP50 from the liquid and then established genetic analysis procedures using RNA extraction, RT-PCR, and qRT-PCR (Appendix F).

A mitochondrial toxicity gene used is *drp-1*. Meyer et al. (2017) and Kim et al. (2018) have used *drp-1,* which provides comparison to other toxicity studies. Pharyngeal pumping genes used were *eat-2, eat-18,* and *egl-19.* (Avery and You 2018). *Eat-2* and *eat-18* are related to the nicotinic acetylcholine receptor and are necessary for rapid pharyngeal pumping. *Egl-19* is related to the L-type calcium channel that regulates all muscle excitation and contraction (Avery and You 2018). *Spe-6* was also tested as a preliminary study suggested reproductive toxicity impacts upon GenX exposure.

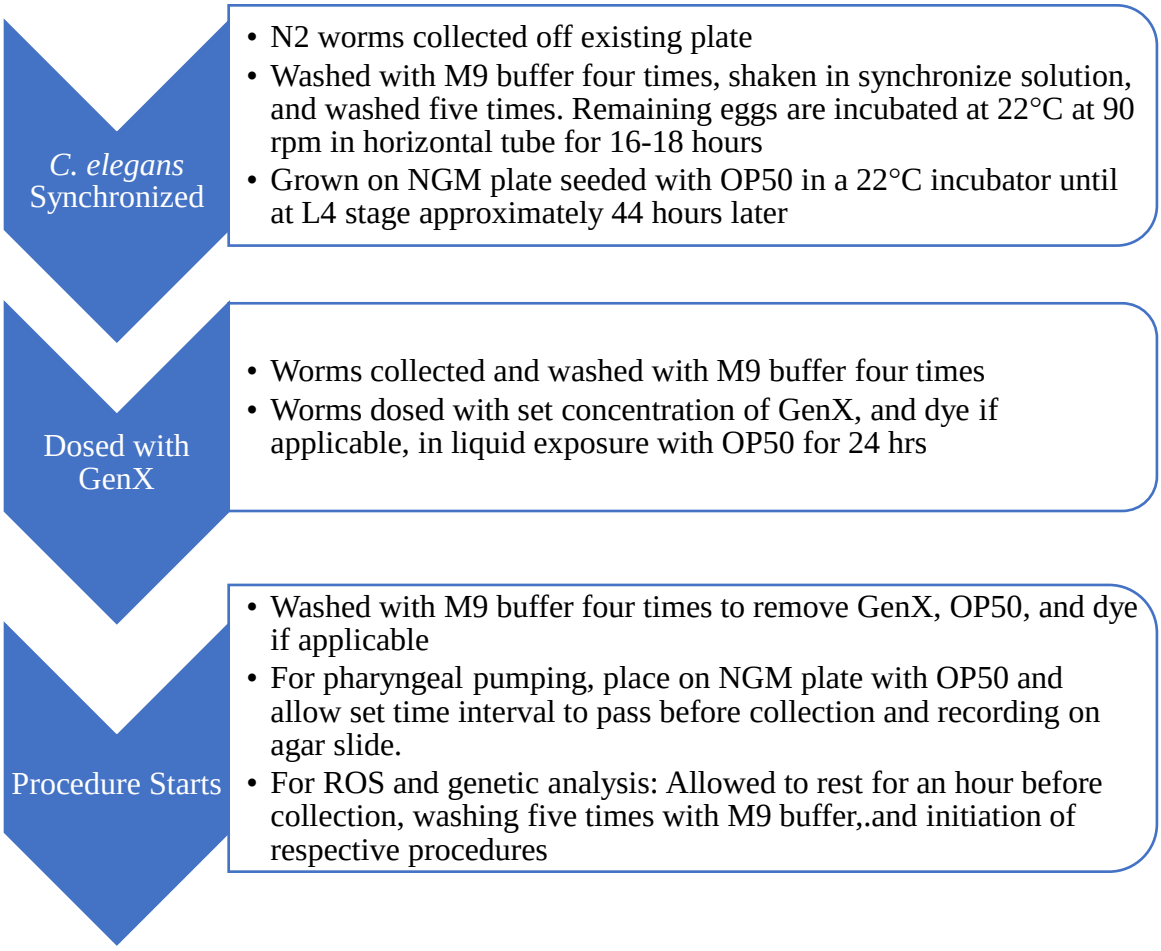

Figure 4. Vertical chevron list of different methods' timelines

Data Analysis

For ROS, data analysis was conducted with SAS Enterprise Guide 8.3. Linear regression ANOVAs with least squared means post-hoc tests were selected to analyze the statistical differences among treatment levels with the significance level of $p<0.05$ and Tukey-Kramer test. Linear regression was chosen to compare the control and three treatments and allow for pairwise comparison with a conservative approach in rejecting the null hypothesis. Additionally, the Tukey-Kramer method tends towards conservative in uneven sample sizes, which avoids Type I errors from occurring due to the different observations of the treatments in the mitochondrial reactive oxygen species fluorescence experiments (Hayter 1984).

After the genes of interests were run through for RNA extraction, RT-PCR, and qRT-PCR (Appendix F) with a minimum of three biological replicates per treatment. Individual replicate samples were removed as an outlier if they fell outside of two standard deviations of the mean. The removal of outliers outside of two standard deviations was used to eliminate the influence of a data point falling outside of the 95th percentile on the calculation of an average from the data present. The replicates from the qRT-PCR plate were then averaged by RT-PCR sample to prevent pseudoreplication (Hulbert 1984) from occurring since the replicates from the same RT-PCR origin sample were not independent from each other.

Fold change was calculated using the formula below (Formula 1) to calculate the change in regulation as compared to control for each sample concentration:

$$\frac{1}{2^{Treatment\ Ct - Control\ Mean}} = Fold\ change$$

Formula 1. Fold change formula for calculating fold change of a sample

Results

Pharyngeal Pumping Behavior Assay

After 24 hours of GenX exposure, the average pumping rate for control, 14, 140, 700, 1,400, 7000, 14,000, and 71,000 ng/L were 167, 199, 217, 239, 180, 201, 210, and 177 times per minute, respectively (Figure 4). Compared to the vehicle control, the pumping rates were significantly increased in 14, 140, 700, 1,400, 7,000, and 14,000 ng/L GenX treatment groups by 19% ($p<0.001$), 30% ($p<0.001$), 43% ($p<0.001$), 8% ($p<0.05$), 20% ($p<0.001$), and 26% ($p<0.001$), respectively.

After 48 hours of GenX exposure, the average pumping rate for control, 14, 140, 700, 1,400, 7000, 14,000, and 71, 000 ng/L were 167, 266, 237, 254, 177, 187, 185, and 197 times per minute, respectively (Figure 5). Compared to the vehicle control, the pumping rates were significantly increased in 14, 140, 1,400, 7,000, 14,000, and 71,000 ng/L GenX treatment groups by 59% ($p<0.001$), 42% ($p<0.001$), 52% ($p<0.001$), 12% ($p<0.01$), 11% ($p<0.05$), and 18% ($p<0.001$), respectively.

After 72 hours of GenX exposure, the average pumping rate for control, 14, 140, 700, 1,400, 7000, 14,000, and 71,000 ng/L were 212, 248, 241, 267, 224, 226, 199, and 200 times per minute (Figure 6). Compared to the vehicle control, the pumping rates were significantly increased in 14, 140, 700, 1,400, and 7,000 ng/L GenX treatment groups by 17% ($p<0.001$), 14% ($p<0.001$), 26% ($p<0.001$), 6% ($p<0.05$), and 7% ($p<0.05$), respectively. On contrast, the pumping rates were significantly decreased in 14,000 and 71,000 ng/L treatment groups by 6% ($p<0.05$) and 6% ($p<0.05$), respectively.

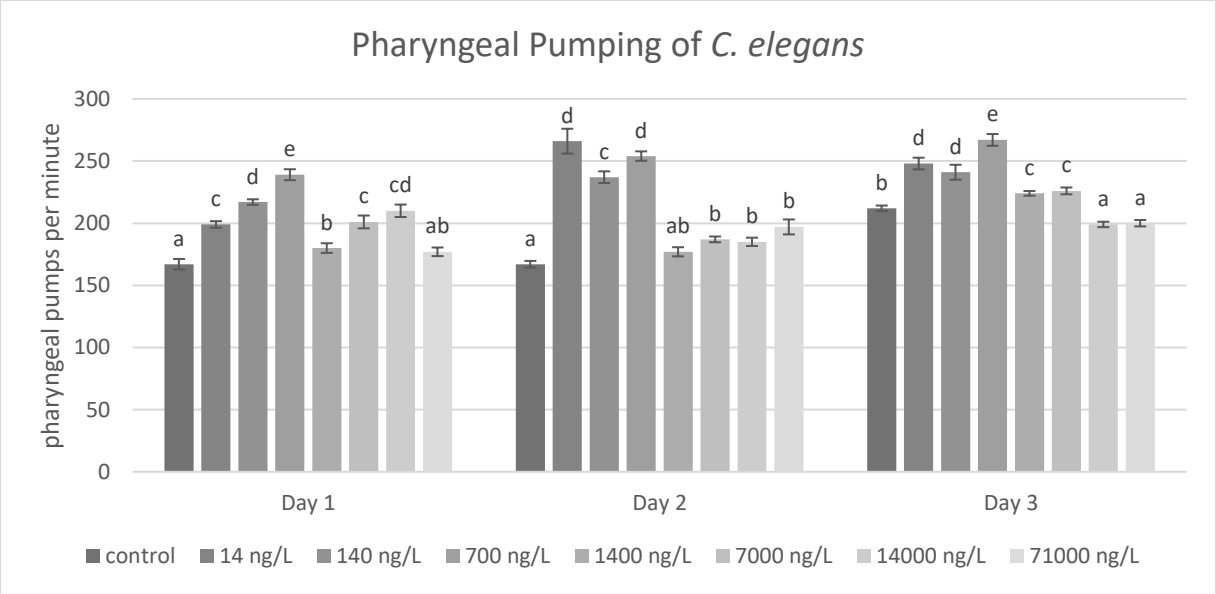

Figure 5. Means of pharyngeal pumps per treatment and timepoint post-treatment

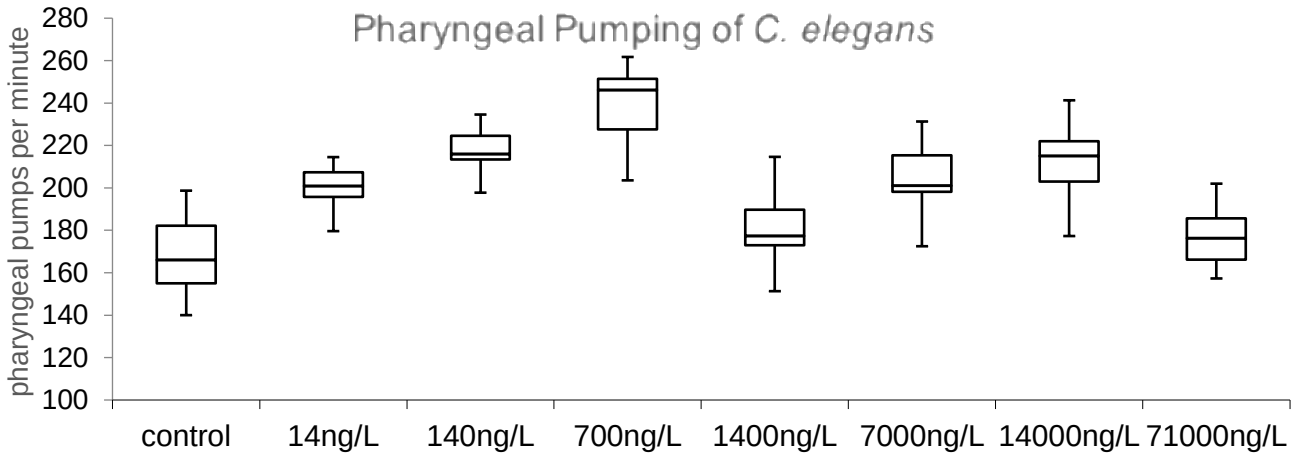

Figure 6. Box-and-whisker chart of pharyngeal pumps per minute 24 hours post-treatment.

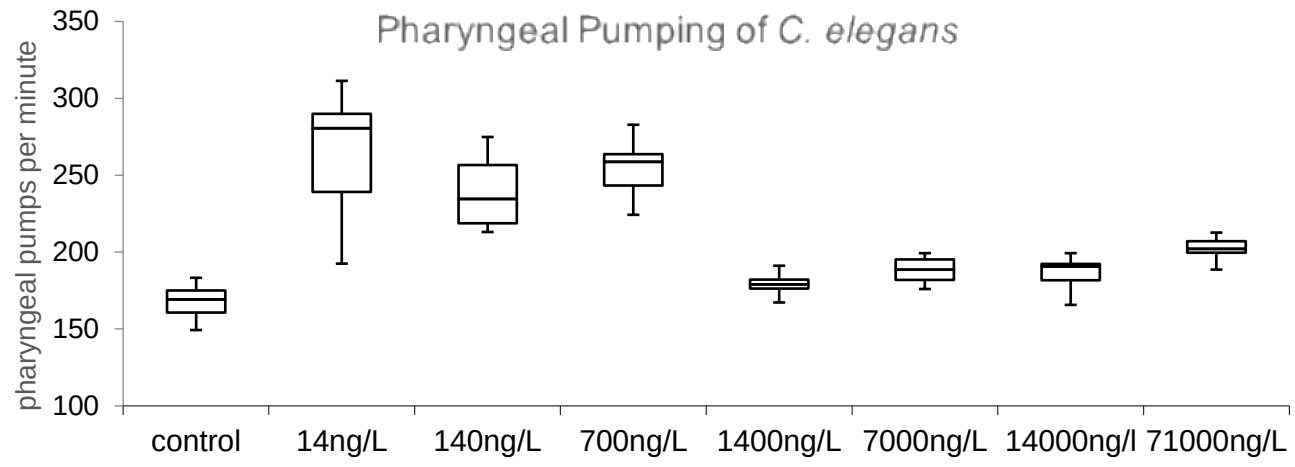

Figure 7. Box-and-whisker chart of pharyngeal pumps per minute 48 hours post-treatment.

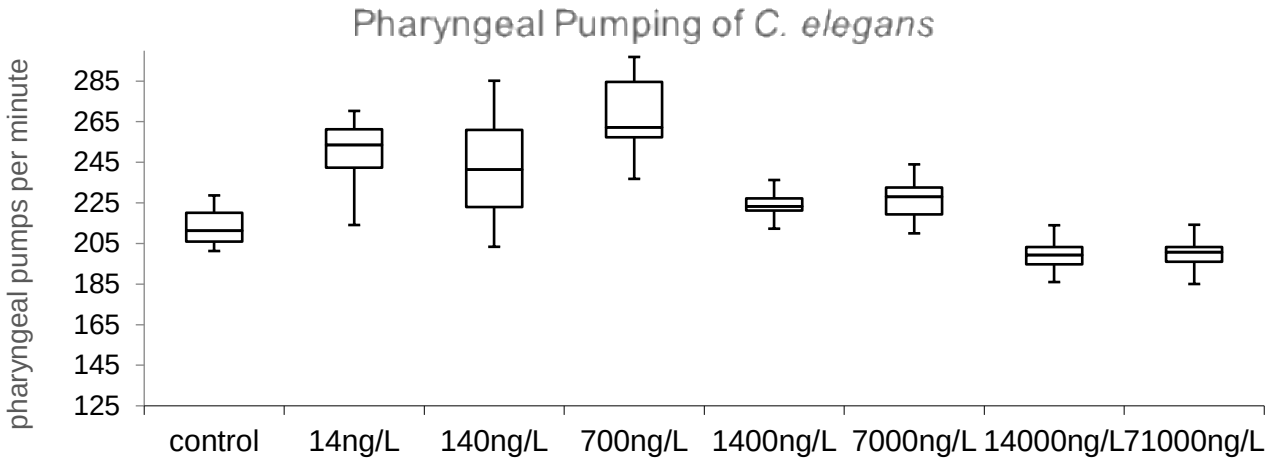

Figure 8. Box-and-whisker chart of pharyngeal pumps per minute 72 hours post-treatment.

Mitochondrial Reactive Oxygenation Species

The fluorescence intensity of the metacarpus, terminal bulb, and whole pharynx were measured as regions of interest. Compared with control, the fluorescence intensity of the first bulb was decreased in the 14 ng/L and 140 ng/L treatment groups by 12.1% and 30.3%, respectively. The decrease in the 140 ng/L group was statistically significant ($p<0.0459$). The ROS fluorescence intensity of the first bulb was increased by 3.5 % in the 700 ng/L group, but the increase is not significant. Compared with control, the fluorescence intensity of the terminal

bulb was decreased in the 14 ng/L and 140 ng/L treatment groups by 2.6% and 26%, respectively. The 700 ng/L treatment caused an insignificant increase of 2%. Within the overall pharynx, the 14 ng/L and 140 ng/L treatments decreased fluorescence by 10.1% and 28.5%, respectively, and 700 ng/L increased fluorescence by 2.2%.

Treatment 140 ng/L was the only treatment significantly different from the control group. The treatment significantly decreased mean fluorescent intensity in the metacorpus ($p<0.0459$) (Appendix H1) and overall pharyngeal pump ($p<0.0391$) (Appendix H2). No significance differences were found in assessing the terminal bulbs between the other different treatments nor the control ($0.1092<p<0.9971$).

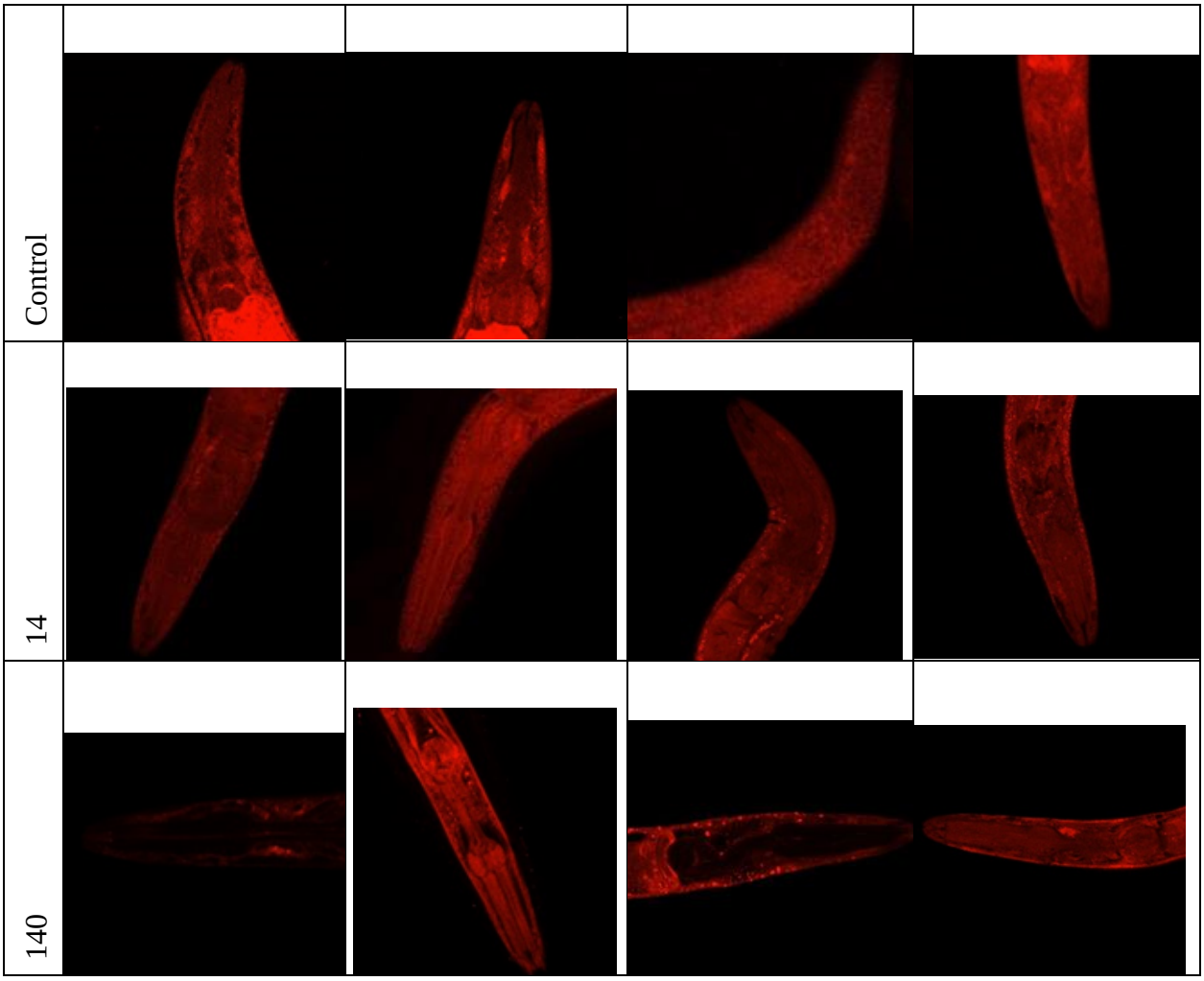

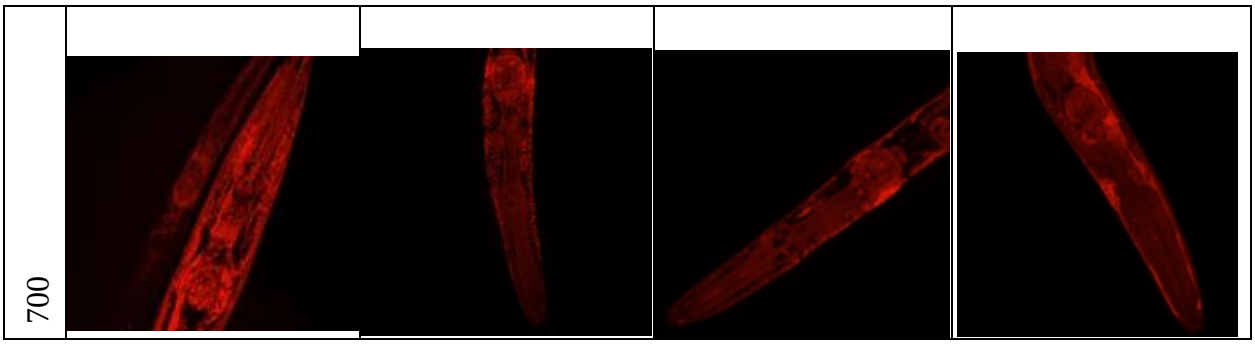

Figure 9. Select representations of mitochondrial reactive oxygen species images

Genetic Analysis

Compared with control, *drp-1* was down regulated > 2-fold in 140 ng/L treatment group. The *eat-18* gene displayed >2-fold upregulation in all treatment groups: 14, 140, and 700 ng/L. The *egl-19* gene was upregulated > 2-fold in 140 ng/L treatment. Last, *spe-6* was upregulated > 2-fold in all treatment groups. Statistically, *eat-18* was the only gene with significant results in significant upregulation and differentiation of treatment. Compared to control, the significant differentiations were 14 ng/L ($p<0.0007$), 140 ng/L ($p<0.0011$), and 700 ng/L group ($p<0.0007$).

Using ANOVA general linear analysis with Tukey adjustment, *drp-1* was not significant at 14 ng/L ($p<0.766$), 140 ng/L ($p<0.323$), or 700 ng/L ($p<0.383$) compared to the control. The general linear model did not significantly fit (F-value = 1.34, $p<0.2931$).

The general linear model fit *eat-18* with great significance (F-value = 21.79, $p<0.0003$). *Eat-18* was not significant at 14 ng/L ($p<1.0$) or 140 ng/L ($p<0.966$), but 700 ng/L was determined to be significant ($p<0.0007$) after Tukey adjustment.

Egl-19 did not significantly fit the general linear model (F-value = 1.07, $p<0.402$). 14 ng/L ($p<0.998$), 140 ng/L ($p<0.537$), and 700 ng/L ($p<0.995$) were not found to be significant.

Spe-6 did not significantly fit the general linear model (F-value = 1.78, $p<0.201$). 14 ng/L ($p<0.167$), 140 ng/L ($p<0.486$), and 700 ng/L ($p<0.509$) were not determined to be significant.

Gene	14 ng/L GenX	140 ng/L GenX	700 ng/L GenX
Drp-1	0.905	0.436	0.598
Eat-18	8.377	70.730	1018.031
Egl-19	0.785	3.304	1.470
Spe-6	110.166	80.240	84.173

Figure 10. Genes of interest and fold change means

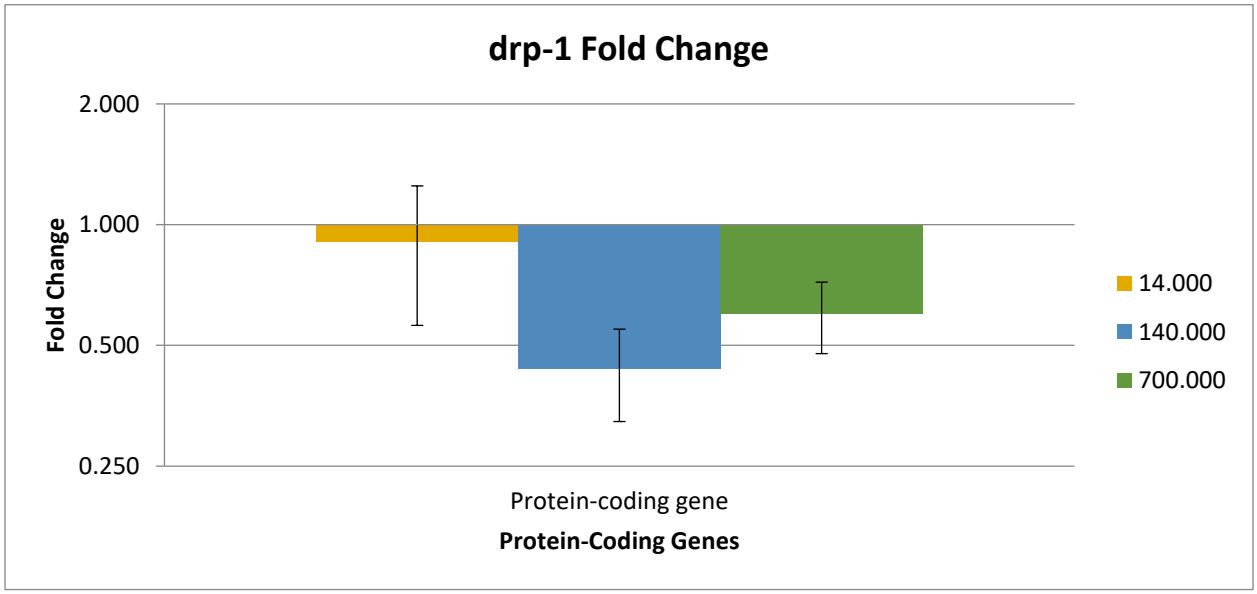

Figure 11. *Drp-1* fold change means of 14, 140, and 700 ng/L of GenX

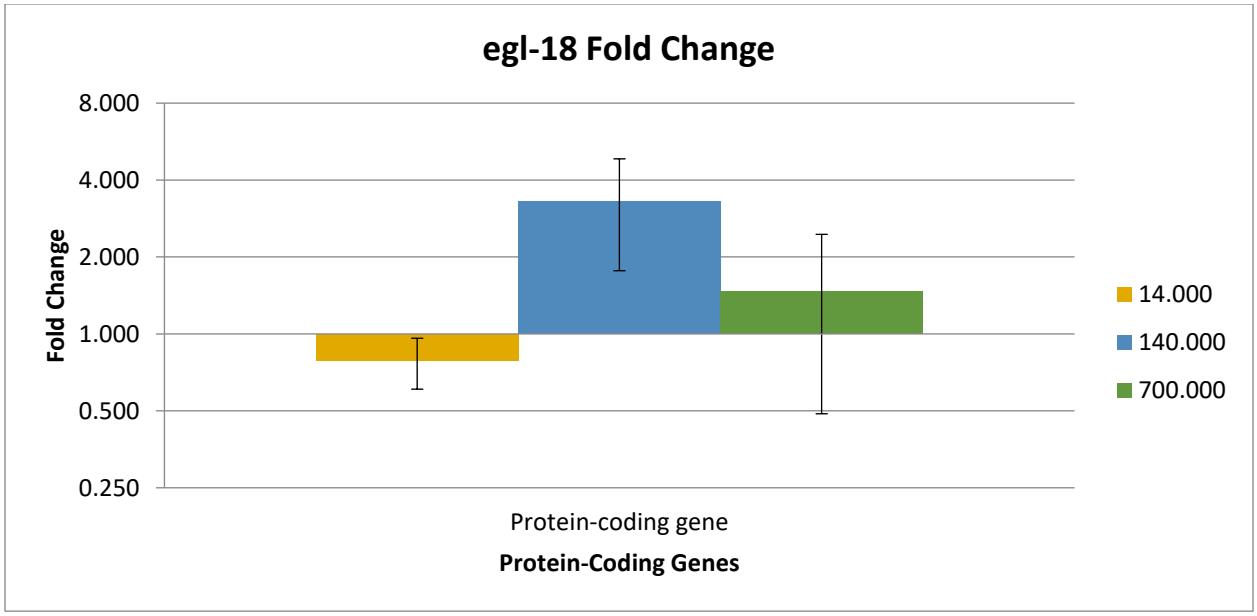

Figure 12. *Egl-19* fold change means of 14, 140, and 700 ng/L of GenX

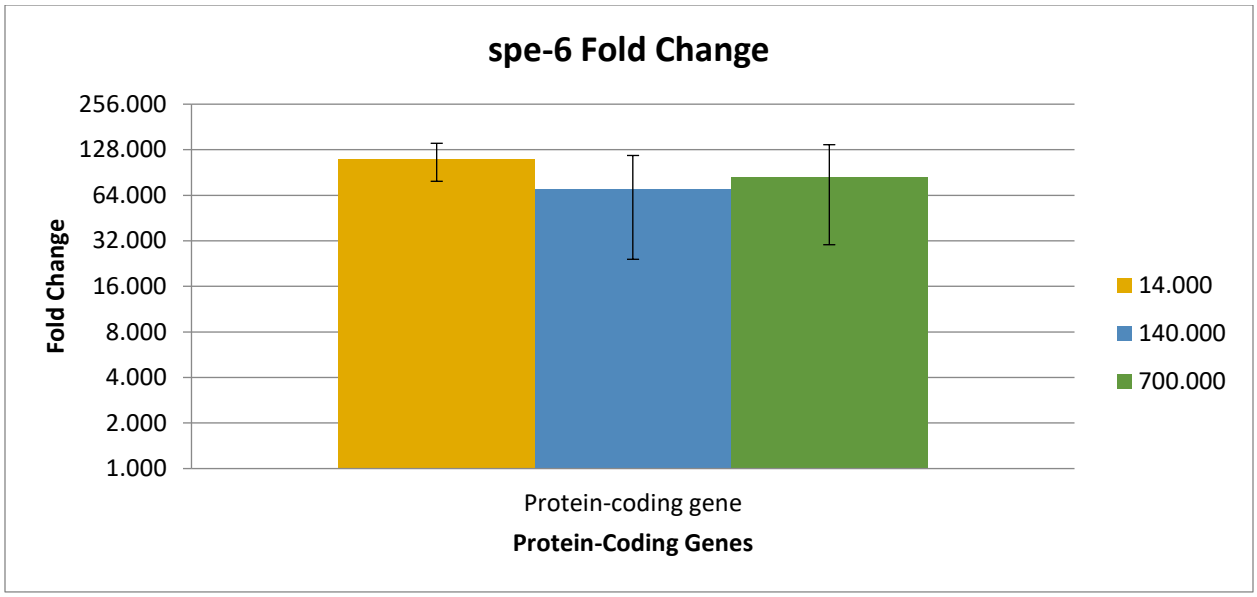

Figure 13. *Spe-6* fold change means of 14, 140, and 700 ng/L of GenX

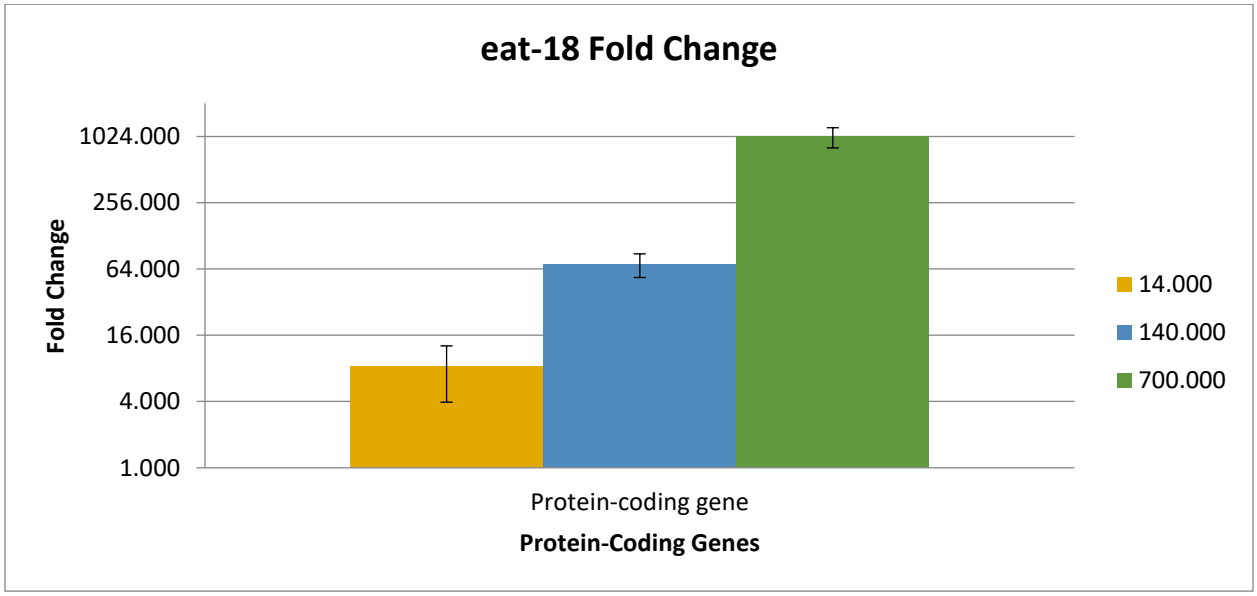

Figure 14. *Eat-18* fold change means of 14, 140, and 700 ng/L of GenX

Discussion

The aims of the thesis were to develop a better understanding of the effects of GenX as a potential toxicant becoming more frequent in the environment and its exposure to humans. Neurological toxicity behavior in the form of pharyngeal pumping was used to determine if the excitatory effects of legacy PFAS apply to GenX and were found to have significantly substantive evidence. Potential symptoms mitochondrial toxicity in the form of semi-quantitative recordings of reactive oxygenation species and genetic analysis of genes of interest were assessed as well with areas of further investigation identified.

This study shows statistical differences in the pharyngeal pumping rate between control and majority of the treatment levels across all cross-sectional timepoints. Pharyngeal pumping had a sensitive response to GenX exposure, and the stimulatory effect of GenX on pharyngeal pumping is consistent across most treatment groups. At the first testing time point of 24 hr post-treatment, the pumping rate was increased significantly, even at the lowest dosage group of 14 ng/L. The pumping rate was significantly increased in six out of seven treatment groups at 24-hour post-treatment and significantly increased in six and five treatment groups at the 48 and 72 hour post-treatment, respectively. Although the extent of the increase did not follow a dose-response relationship across the whole dosage range, at the 24- hour post-treatment the pumping rate is increased by 19% to 30% and then to 43% for 14, 140, and 700 ng/L treatment groups, indicating dose-response relationship may exist in a relatively narrow dosage range.

Temporal response patterns were shown in some dosage groups. In 14 ng/L group, the pumping rate was increased by 19% compared to control at the 24-hour post-treatment point time and then increased further by 59% at the 48 hour post-treatment. Similarly in 140 and 700 ng/L treatment groups, the pumping rates were increased until 48 hour post-treatment time point. The

pumping rate increases in the higher dosage ranges of 7,000 to 71,000 ng/L were not as significant as the lower dosage range of 14 to 700 ng/L. The result indicates that cytotoxic effects may offset some of the stimulatory effects in higher dosages and potentially time as well. While five treatment groups still displayed significant higher pumping rate as compared to control at 72-hour post-treatment, the increases were not as significant as the 24- and 48-hour time points, suggesting a tendency to return to normal as the recovery time prolongs.

Pharyngeal pumping is associated with M1, M2, M3, M4, MC, MI motor neurons, NSM neurosecretory neurons, and I1, I2, I3, I4, I5, I6 interneurons (WormAtlas et al. 2018), and multiple genes are associated with pharyngeal pumping mechanisms (WormAtlas et al. 2018). Many of these genes code for the same or similar receptor proteins. Additionally, like the heart in higher organisms, the *C. elegans* pharynx is a neuromuscular pump that responds to a variety of neural and myoid regulators including neurotransmitters and neurohormonal and enteric signals with classic neurotransmitters including acetylcholine, glutamate, and serotonin also supporting a higher pumping rate in *C. elegans* (Hall and Altum 2008). *Eat-18* and eat-2 are interactor overlapping genes (WormBase). *Eat-18* codes for a small single-pass transmembrane protein, EAT-18, expressed in the pharyngeal muscle, likely by directly binding to the nicotinic acetylcholine receptor EAT-2 for which EAT-18 is necessary for the proper targeting or function of most or all of them. EAT-18 is necessary for M4 to TB muscle transmissions while EAT-2 is thought to be less necessary (Avery and You, 2018).

The mechanism of GenX-induced high pumping rate is currently unclear. In other PFAS studies, long-chained PFAS were found to increase acetylcholine in chordates and invertebrates (Yuan et al. 2018; Foguth et al. 2020). GenX may act upon one of the acetylcholine receptors or generate a similar excitatory signal as legacy PFAS have done. The upregulation at 700 ng/L for

eat-18 indicates that EAT-18 is being produced in higher concentration, causing the increase in pharyngeal pumping. Investigation into genes related to other neurotransmitters would provide a better understanding of the mechanisms causing hyperactivity in greater detail.

The lack of significant results from *egl-19* indicates that the gene related to the calcium channel regulating muscle excitation and contraction of *C. elegans* (Avery and You 2018) is not affected by the tested range of GenX dosages. The result provides support that human orthologs implicated in Brugada syndrome 3, Timothy syndrome, and multiple X-linked recessive diseases (WormBase 2023) are not expected to result from exposure to GenX. Similarly, the lack of significant response to the range of GenX dosages tested in *drp-1* indicates that the human ortholog gene DNM1L and genes implicated in several diseases including Alzheimer's disease, defective mitochondrial and peroxisomal fission-related encephalopathy, optic atrophy, and pulmonary fibrosis (WormBase 2023) are potentially not affected by exposure to GenX.

The conservative skewing of Tukey adjustment may account for the discrepancy between high fold changes but insignificant differences. A higher replicate count with even treatment numbers would allow for adjustment based on arithmetic means rather than least squares means may cause *egl-19* to become statistically significant with $p<0.05$ remaining as the Type 1 test. Evaluating the genes of interest that indicate significance and potential significance based on fold change means, as well as evaluating mitochondrial genes to assess mitochondrial toxicity, would be valuable in assessing GenX effects as an environmental toxicant and potential alternative genetic expressions.

The reactive oxygen species fluorescence results were not as expected. Energy demanding neurons and muscle cells like those in *C. elegans* pharynx contain high mitochondria volumes. Mitochondria are the major generator of endogenous reactive oxygen species (ROS)

including superoxide anions, hydrogen peroxide, and hydroxyl radicals (Zang et al. 2014). Superoxide anions can be converted to hydrogen peroxide by the mitochondrial superoxide dismutase, a process conserved from nematodes to higher organisms. According to the free radical theory of aging, increased respiration and oxygen consumption will result in increased mitochondrial ROS production and consequent cellular damages (Zang et al. 2014) Although it is hypothesized that enhanced pharyngeal pumping should require more energy and thus increased mitochondrial respiration and oxygen consumption, the MitoSOX Red staining findings did not suggest an increase in mitochondrial ROS production. It is possible that GenX facilitates effective energy expenditure of cells that allows for high energy production without excessive ROS resulting. Performing the experiment again with more experience of the procedure, positive and negative controls, and assessment of fluorescent measurement methods would provide more insight into the precision of the results.

While a trend of reactive oxygenation species did not emerge in response to the increase in pharyngeal pumping, the significant decrease in ROS at the 140 ng/L treatment level is worth evaluating further to understand what reaction may be occurring to cause a decrease and determine if the mechanism. In the pharyngeal pumping results, exposures higher than 700 ng/L (14,000 ng/L, 7,000, 14,000, and 71,000 ng/L) across all timepoints resulted in a decrease in pumping. The drop in trend is possibly due to a stress response (Bar-Ziv et al. 2020). An unfolded protein response of the mitochondria and/or an oxidative stress response would potentially explain the reduction of activity at the expose dose rising above the levels found in the Cape Fear River Basin. Further research into mechanisms evaluating the response is needed however to determine.

In future experiments, some changes would improve the quality of the research. Preforming a lifespan assessment would allow evaluation of the effects of toxicant exposure on long-term survival. If the lifespan of the *C. elegans* is shorter than control, the expenditure of energy from increased pharyngeal pumping supports the theory of reactive oxygen species on aging. The lack of significant increases in reactive oxygen species fluorescence is potentially from effective reactive oxygen species usage. A significantly shortened or lengthened lifespan compared to a control would allow for a better concept of the effects on the overall health of the *C. elegans* in the broader conceptualization. In the reactive oxygen species experiment, the positive control of paraquat should be used (Ray et al. 2015) to allow comparison between a positive control and the treatments. EtAc as a negative control also would be recommended in future experiments to reference (Ray et al. 2015).

Similarly, assessing the potential for inheritable mitochondrial damage from GenX in *C. elegans* throughout generations would provide insight into the effects from long-term in parent organisms (Gorman et al. 2015). Providing a low dosage during L1 stage to L4 stage development would simulate changes in a developing organism. In this manner, the potential of GenX acting as a development toxicant in *C. elegans* as it had in pregnant rats in Conley et al. (2021) may be assessed. Testing the effects of GenX during *C. elegans* development may provide a useful assessment for its own sake. Combining the experiment with syncing laid eggs from the exposed parents and testing changes in mitochondria using lifespan assessment, mitochondrial morphology, ROS fluorescence, and genetic changes would provide insight into the long-term effects of GenX as a mitochondrial toxicant with the future to impact future generations.

In addition, the significant decrease in reactive oxygen species at 140 ng/L in the metacorpus and pharynx as a whole is worth investigating. In the 48- and 72-hour time points of pharyngeal pump data, a decrease in the trend at 140 ng/L occurred (Figure 6; Figure 7). The decrease at 140 ng/L may indicate a rescue mechanism is occurring within the *C. elegans* to correct for effects of GenX in longer time points of exposure. The difference in scale between the potential rescue response at 140 ng/L and at concentrations higher than 700 ng/L implies that the highest dosages cause a shutdown while 140 ng/L cause efforts to mitigate before the trend increases with 700 ng/L. The peculiarity is another question worth understanding.

While the study itself is only a small contribution to the larger effort to identify potential effects of GenX and the diminutive forms created in its degradation, the research provides a basis for further research into mitochondrial toxicity of GenX in particular and GenX as a toxicant as a whole before the chemical grows to wider usage with potentially similar harm created as the legacy long-chained PFAS before it. With the potential effects described comes the reality that human exposure for several years has already occurred within communities without scientific evidence to justify the commercial claims of no harm from widespread exposure. While results in the study indicate that GenX may cause significant effects with human exposure, the uncertainty from the lack of research has already caused fear in exposed residents of communities. Further research remains necessary to either dispel the uncertainty or provide answers for what is to be expected in short- and long-term health effects from exposure. In addition, the research provides new fields into mitochondrial toxicity worth investigating to understand the mechanisms involved in dosage response.

References

Avery L, Horvitz HR. 1989. Pharyngeal pumping continues after laser killing of the pharyngeal nervous system of C. elegans. Neuron. 3: 473–485.

Avery L, You YJ. *C. elegans* feeding. In: WormBook: The Online Review of *C. elegans* Biology [Internet]. Pasadena (CA): WormBook; 2005-2018. Available from: https://www.ncbi.nlm.nih.gov/books/NBK116080/

Bankhead P. 2014. Analyzing fluorescence microscopy images with ImageJ. Available from: https://confocal.uconn.edu/wp-content/uploads/sites/1081/2016/02/2014-05_Analyzing_fluorescence_microscopy_images.pdf

Bar-Ziv R, Frakes AE, Higuchi-Sanabria R, Bolas T, Frankino PA, Gildea HK, Metcalf MG, Dillin A. 2020. Measurements of physiological stress responses in *C. elegans*. J Vis Exp. 159: 10.3791/61001. doi: 10.3791/61001. PMID: 32510480; PMCID: PMC7840273.

Bernstein SA, Morley GE. 2006. Gap junctions and propagation of the cardiac action potential. Adv. Cardiol. 42: 71–85.

Blake BE, Cope HA, Hall SM, Keys RD, Mahler BW, McCord J, Scott B, Stapleton HM, Strynar MJ, Elmore SA, Fenton SE. 2020. Evaluation of maternal, embryo, and placental effects in CD-1 mice following gestational exposure to perfluorooctanoic acid (PFOA) or hexafluoropropylene oxide dimer acid (HFPO-DA or GenX). Environmental Health Perspectives. 128(2): https://doi.org/10.1289/EHP6233

Boyd WA, Smith MV, Freedman JH. 2012. Caenorhabditis elegans as a model in developmental toxicology. Methods Mol Biol. 889:15-24. doi:10.1007/978-1-61779-867-2_3

Brase RA, Mullin EJ, Spink DC. 2021. Legacy and emerging per- and polyfluoroalkyl substances: analytical techniques, environmental fate, and health effects. Int. J. Mol. Sci. 22: 995. https://doi.org/10.3390/ijms22030995

Brendel S, Fetter É, Staude C, Vierke L, Biegel-Engler A. 2018. Short-chain perfluoroalkyl acids: environmental concerns and a regulatory strategy under REACH. Environ. Sci. Eur. 30(1): 9. doi: 10.1186/s12302-018-0134-4

Caldwell KA, Thies JL, Caldwell GA. 2018. No country for old worms: a systematic review of the application of *C. elegans* to investigate a bacterial source of environmental neurotoxicity in Parkinson's Disease. Metabolites. 8:70. doi:10.3390/metabo8040070.

Cannon RE, Richards AC, Trexler AW, Juberg CT, Sinha B, Knudsen GA, Birnbaum LS. 2020. Effect of GenX on P-glycoprotein, breast cancer resistance protein, and multidrug resistance-associated protein 2 at the blood-brain barrier. Environ. Health Perspect. 128: 37002.

Chen FJ, Wei CY, Chen QY, Zhang J, Wang L, Zhou Z, Chen MJ, Liang Y. 2018. Internal concentrations of perfluorobutane sulfonate (PFBS) comparable to those of perfluorooctane sulfonate (PFOS) induce reproductive toxicity in *Caenorhabditis elegans*. Ecotoxicol. Environ. Saf. 158: 223–229.

Chen J-N, Fishman MC. 1996. Zebrafish tinman homolog demarcates the heart field and initiates myocardial differentiation. Development. 122: 3809-3816.

CompTox Chemicals Dashboard v2.2.1. Ammonium perfluoro-2-methyl-3-oxahexanoate. Environmental Protection Agency. https://comptox.epa.gov/dashboard/chemical/details/DTXSID40108559. Accessed on June 28, 2022.

Conley JM, Lambright CS, Evans N, McCord J, Strynar MJ, Hill D, Medlock-Kakaley E, Wilson VS, Gray LEG II. 2021. Hexafluoropropylene oxide-dimer acid (HFPO-DA or GenX) alters maternal and fetal glucose and lipid metabolism and produces neonatal mortality, low birthweight, and hepatomegaly in the Sprague-Dawley rat. Environment International. 146: 106204.

Corton JC, Cunningham ML, Hummer BT, Lau C, Meek B, Peters JM, Popp JA, Rhomberg L, Seed J, Klaunig JE. 2014. Mode of action framework analysis for receptor-mediated toxicity: The peroxisome proliferator-activated receptor alpha (PPARα) as a case study. Critical Reviews in Toxicology. 44(1): 1-49. DOI: 10.3109/10408444.2013.835784

Dröge W. 2002. Free radicals in the physiological control of cell function. Physiol Rev. 82(1): 47-95. doi: 10.1152/physrev.00018.2001.

Foguth R, Sepúlveda MS, Cannon J. 2020. Per- and polyfluoroalkyl substances (PFAS) neurotoxicity in sentinel and non-traditional laboratory model systems: potential utility in predicting adverse outcomes in human health. Toxics. 8:42. doi:10.3390/toxics8020042

Gaballah S, Swank A, Sobus JR, Howey XM, Schmid J, Catron T, McCord J, Hines E, Strynar M, Tal T. 2020. Evaluation of developmental toxicity, developmental neurotoxicity, and tissue dose in zebrafish exposed to GenX and other PFAS. Environ. Health Perspect. 128:4.

Gorman GS, Schaefer AM, Ng Y, Gomez N, Blakely EL, Alston CL, Feeney C, Horvath R, Yu-Wai-Man P, Chinnery PF, Taylor RW, Turnbull DM, McFarland R. 2015. Prevalence of nuclear and mitochondrial DNA mutations related to adult mitochondrial disease. Ann. Neurol. 77(5): 753–759.

Greaves AK, Letcher RJ. 2013. Linear and branched perfluorooctane sulfonate (PFOS) isomer patterns differ among several tissues and blood of polar bears. Chemosphere. 93: 574-580.

Hall DH, Altun ZH. 2008. *C. elegans* atlas. 1st ed. Cold Spring Harbor (NY): Cold Spring Harbor Laboratory Press. Chapter 5: Muscle System; p. 145-188. ISBN: 9780879697945.

Hayter AJ. 1984. A proof of the conjecture that the Tukey-Kramer multiple comparisons procedure is conservative. The Annals of Statistics, 12(1): 61-75. https://doi.org/10.1214/aos/1176346392

Hobson RJ, Geng J, Gray AD, Komuniecki RW. 2003. SER-7b, a constitutively active Galphas coupled 5-HT7-like receptor expressed in the *Caenorhabditis elegans* M4 pharyngeal motor neuron. J. Neurochem. 87: 22–29.

Hopkins ZR, Sun M, DeWitt JC, Knappe DR. 2018. Recently detected drinking water contaminants: GenX and other per- and polyfluoroalkyl ether acids. J Am Water Works Assoc, 110: 13-28. doi:10.1002/awwa.1073

Houck KA, Patlewicz G, Richard AM, Williams AJ, Shobair MA, Smeltz M, Clifton MS, Wetmore B, Makarov S. 2021. Bioactivity profiling of per- and polyfluoroalkyl substances (PFAS) identifies potential toxicity pathways related to molecular structure. Toxicology. 457: 152789.

Huan C, Alexander J, Stainier DY, Okkema PG. 1998. Rescue of Caenorhabditis elegans pharyngeal development by a vertebrate heart specification gene. Proc. Natl. Acad. Sci. USA. 95: 5072-5075.

Hulbert SH. 1984. Pseudoreplication and the design of ecological field experiments. Ecological Monographs. 54(2): 187-211.

Jabeen M, Fayyaz M, Irudayaraj J. 2020. Epigenetic modifications, and alterations in cell cycle and apoptosis pathway in A549 lung carcinoma cell line upon exposure to perfluoroalkyl substances. Toxins. 8:112.

Kim H, Perentis RJ, Caldwell GA, Caldwell KA. 2018. Gene-by-environment interactions that disrupt mitochondrial homeostasis cause neurodegeneration in *C. elegans* Parkinson's models. Cell Death & Disease. 9:555. doi:10.1038/s41419-018-0619-5

Mango SE. 2007. The *C. elegans* pharynx: a model for organogenesis, WormBook, ed. The C. elegans Research Community WormBook. doi:10.1895/wormbook.1.129.1. http://www.wormbook.org.

Meyer JN, Hartman JH, Mello DF. 2018. Mitochondrial toxicity. Toxicological Sciences. 162(1): 15–23. doi:10.1093/toxsci/kfy008

North Carolina Department of Health and Human Safety. 2018. GenX Frequently Asked Questions. https://files.nc.gov/ncdeq/GenX/FAQ_updated_100417-5.pdf

Okkema PG, Ha E, Haun C, Chen W, Fire A. 1997. The *Caenorhabditis elegans* NK-2 homeobox gene ceh-22 activates pharyngeal muscle gene expression in combination with pha-1 and is required for normal pharyngeal development. Development 124: 3965–3973.

Pasetto S. 2022. Instructions for Zeiss LSM 800 Confocal Microscope. East Carolina University Biology Department – Imaging Core Facility.

Ray A, Martinez BA, Berkowitz LA, Caldwell GA, Caldwell KA. 2014. Mitochondrial dysfunction, oxidative stress, and neurodegeneration elicited by a bacterial metabolite in a C. elegans Parkinson's model. Cell Death & Disease. 5: e984. https://doi.org/10.1038/cddis.2013.513

Sammi SR, Foguth RM, Nieves CS, De Perre C, Wipf P, McMurray CT, Lee LS, Cannon JR. 2019. Perfluorooctane sulfonate (PFOS) produces dopaminergic neuropathology in *Caenorhabditis elegans*. Toxicol. Sci. 172: 417–434.

Sarasija S, Norman KR. 2018. Analysis of mitochondrial structure in the body wall muscle of *Caenorhabditis elegans*. Bio Protoc. 8(7): e2801. doi: 10.21769/BioProtoc.2801

Smith RL, De Vos WH, de Boer R, Manders EMM, van der Spek H. 2015. Chapter 26: In vivo visualization and quantification of mitochondrial morphology in *C. elegans*. Volkmar Weissig and Marvin Edeas (eds.). Mitochondrial Medicine: Volume II, Manipulating Mitochondrial Function. Methods in Molecular Biology, vol. 1265. DOI 10.1007/978-1-4939-2288-8_26.

Strynar M, Dagnino S, McMahen R, Liang S, Lindstrom A, Andersen E, McMillan L, Thurman M, Ferrer I, Ball C. 2015. Identification of novel perfluoroalkyl ether carboxylic acids (PFECAs) and sulfonic acids (PFESAs) in natural waters using accurate mass time-of-flight mass spectrometry (TOFMS). Environ. Sci. & Technol. 49(19): 11622. https://doi.org/10.1021/acs.est.5b01215

Thompson CM, Fitch SE, Ring C, Rish W, Cullen JM, Haws LC. 2019. Development of an oral reference dose for the perfluorinated compound GenX. J Appl Toxicol. 39: 1267-1282.

US EPA. 2000. EPA and 3M announce phase out of PFOS. Available online: https://archive.epa.gov/epapages/newsroom_archive/newsreleases/33aa946e6cb11f35852568e1005246b4.html (accessed on 11 October 2021).

WormAtlas, Altun ZF, Herndon LA, Wolkow CA, Crocker C, Lints R, Hall DH. 2002-2021. ed.s. http://www.wormatlas.org

WormBase. 2023. National Human Genome Research Institute. https://wormbase.org/

Yuan Z, Shao X, Miao Z, Zhao B, Zheng Z, Zhang J. 2018. Perfluorooctane sulfonate induced neurotoxicity responses associated with neural genes expression, neurotransmitter levels and acetylcholinesterase activity in planarians *Dugesia japonica*. Chemosphere. 206: 150-156.

Zang QS, Wolf SE, Minei JP. 2014. Sepsis-induced Cardiac Mitochondrial Damage and Potential Therapeutic Interventions in the Elderly. Aging Dis. 5(2):137-49. doi: 10.14336/AD.2014.0500137. PMID: 24729939; PMCID: PMC3966672.

Zheng F, Aschner M, Li H. 2021. Evaluations of environmental pollutant-induced mitochondrial toxicity using *Caenorhabditis elegans* as a model system. Xiaoping Pan and Baohong Zhang (eds.), Environmental Toxicology and Toxicogenomics: Principles, Methods, and Applications, Methods in Molecular Biology, vol. 2326. https://doi.org/10.1007/978-1-0716-1514-0_3

Appendices

Appendix A: Synchronization of *C. elegans* established Dr. Xiaoping Pan Laboratory Methodology

Synchronization solution: 2 mL of NaOH, 5 mL of commercial bleach, 17 mL of autoclaved H2O

1. The *C. elegans* from a strain are collected from established and populated NGM plates seeded with OP50. The plate is held in a tilt and the worms are washed off the plate with 5 mL M9 buffer solution. The worms are pipetted into a 15 mL Falcon tube.
2. The worms are centrifuged and washed with M9 twice. The liquid down to the 1 mL line is removed. M9 is refilled to 5 mL for a complete wash.
3. The M9 in the Falcon tube is reduced to 1 mL. 5 mL of synchronization solution is added to the Falcon tube.
4. The Falcon tube is shaken for 6-10 minutes with the purpose of dissolving adults and leaving only eggs. The state of dissolution is checked beneath a dissecting microscope through the clear plastic tube. Once only eggs remain, the next step is initiated.
5. The eggs within the tube are quickly centrifuged and washed with M9 four times to remove synchronization solution over the course of washes.
6. After five washes, the Falcon tube containing eggs is placed in an incubator for 16 to 18 hours at 21 degrees Celsius at 80-90 rpm. When the eggs have hatched, the lack of food in the solution arrests development. Within the time period, all the eggs will have hatched, and the worms remain in the same development phase of L1. Past the eighteen hour time point, the worms are likely to starve and die.
7. After the 16-18 hour time point, the Falcon tube is centrifuged until only 1 mL of M9 containing the hatched worms remains. A NGM plate is seeded with 25 uL of *E. coli* OP50 as food to prevent starvation stress. The 1 mL containing stage L1 worms are pipetted onto the NGM plate and allowed to grow for 40-44 hours until L4 larval stage had been reached.

Appendix B: Nematode culture and maintenance

M9 buffer: 3 g KH2PO4, 6 g Na2HPO4, 5 g NaCl, 1 ml 1 M MgSO4, H2O to 1 L

K-medium: 2.36 g KCL, 3 g NaCl in 1 L of ddH_2O (Boyd et al. 2012)

NGM plate: 3 g of NaCl, 2.5 g of peptone, 17 g of agar, and 975 mL of ddH_2O

1. Mixed well with a stir bar and then autoclaved at 121°C for 20 minutes.
2. Mixture allowed to cool to 55°C on hot plate with stir bar stirring mixture.
3. Added 1 ml cholesterol (5mg/ml in ETOH), 1 ml $CaCl_2$ (1M), 1 ml of $MgSO_4$ (1M) and 25 ml of potassium phosphate (PH 6) in respective order.
4. The mixture was left to mix at 55°C on hot plate with the use of a stir bar as mixture pipetted into 10 cm petri dishes (25 mL) to cool and solidify before sealing with wax strips.
5. Plates were left under fume hood overnight, and plates were screened to remove any form of growth before storage in 4°C walk-in freezer.

Appendix C: Zheng et al. (2021) "Evaluations of Environmental Pollutant-Induced Mitochondrial Toxicity Using *Caenorhabditis elegans* as a Model System"

Mitochondrial ROS Detection

1. Grow synchronous L4 nematodes on NGM plates spread with OP50 and 10 μM MitoSOX Red for 24 h. (Note: All fluorescent studies are suggested to perform at 20 C in dim light.)

[Make 5 mM of MitoSOX stock solution using one of the ten packaged vials and 13 uL of DMSO. The stock solution becomes the working solution with M9. Dilute to 10uM working solution for exposure by adding 5uL stock:2.5mL M9 or 4uL:2mL M9 solution.

Stock solution should keep if stored at 4C in refrigerator. Working solution keeps in less time.]

2. Collect the young adult nematodes (Note: after 24 h from the above step, the nematodes turn into young adults) and expose with the environmental pollutant of interest.

Recommended Exposure Method:

[Expose 2500 synchronized L4 nematodes (40-44 h after sync) with 25 μL liquid exposure solutions, respectively, in 500 μL reaction system for 2 h at 20 C (Due to the difference in sensitivity and size, 5000 L1 nematodes are roughly equal to 2500 L4 nematodes in 500 μL reaction system containing 25 μL of 20x exposure solutions.).

Remove toxicants with two washes using 85 mM NaCl (If solid exposure is preferred, i.e., the toxicant is mixed in plates for prolonged exposure, the doses should be 10 folds less than liquid exposure.)]

3. Recover the exposed nematodes on NGM plates containing OP50 for 1 h. (Note: This step is also important for the clearance of residual dye in their guts.)

4. Pick the nematodes to a droplet of 1 mM levamisole on the coverslip. (Note: Nematode can be anesthetized by 1 mM levamisole.)

5. Mount the coverslip onto a microscope slide containing a 4% agarose pad.

6. Label strains and conditions of the experiments.

7. Examine fluorescent intensity in the posterior pharyngeal bulb of the nematodes with 510 and 580 nm (excitation/emission) wavelengths.

8. Quantify fluorescent intensity using Fiji software to unveil the effect of environmental toxicants on mitochondrial ROS. (Note: Otherwise, genetic-modified *C. elegans* strains could be used directly, without fluorescent staining. These include nematodes which harbor mitochondrial-targeted roGFP, HyPer, and mt-cpYFP for monitoring redox state changes, peroxide, and superoxide contents, respectively. Those nematodes give instantaneous readouts and fluctuate based on mitochondrial redox levels [19–21]. Furthermore, MitoTimer reporter strain changes fluorescence from green to red under mitochondrial stress, therefore could demonstrate mitochondrial damage under physiological and pathological conditions in vivo [22]).

Mitochondrial Gene Expression and Modifications Assessment

1. Conduct three freeze and thaw cycles on the nematodes with liquid nitrogen to breakdown cuticles and release RNA (2500 L4 nematodes per exposure are adequate for qRT-PCR to generate reproducible results).
2. Isolate mRNA with TRIzol following manufacturer's protocol (Life Technologies, USA).
3. Determine the concentration and purity (A260/A280 and the A260/A230 ratio) of the isolated RNA by a NanoDrop 2000 spectrophotometer.
4. Reverse-transcribe cDNA from RNA using High Capacity cDNA Reverse Transcription kit following manufacturer's protocol. Briefly, prepare 2 x reaction mix using the kit's components according to the protocol. Dilute 1 μg RNA to 10 μL solution with RNase-free water. Then mix the 10 μL of 2 x reaction mix with 10 μL RNA This would result in 0.5 μg of cDNA per 10 μL. The recommended cDNA transcription protocol is: 25 ℃ 10 min, 37 °C 2 h, 85 °C 5 min, and stop at 4 °C.
5. Prepare PCR mix according to Taqman gene-expression assay probes protocol. 3 μL of cDNA generated above is added to 5 μL of the Taqman probles, followed by 1.5 μL water to makeup 10 μL system. The 10 μL system could be scaled up to 50 μL per tube.
6. Run qPCR on the BioRad Real-time system. The recommended qPCR protocol is TaqMan standard protocol (1 h 30 min).
7. Normalize the target gene expression to the relatively stable expression gene tba-1.
8. Determine the relative mRNA levels of gene of interests with the 2--$^{\Delta\Delta CT}$ method.

Appendix D. List of Primers for Genes of Interest. List of genes and their corresponding forward and reverse primers.

Genes	Forward Primer (5'>3')	Reverse Primer (5'>3')
Drp-1	AGTGCGGATGACTGACTGG	GCACGTTGGTTCTGGGATTG
Eat-2	TGTTGGAGGATCAGGCGAAG	ACCTTGTAAGCAGGCGTAGG
Eat-18	CCCAACCTTTCCAGAATGCG	GCTCGGGAACTCGATGACAC
Egl-19	AGGCTGTTAGCATGGTTTGG	TCCAAGAGACACCACACACC
Spe-6	TGGCTTTGTCGAGACGTGAA	CGGGATGATTTTGCCCTCCT

Appendix E: ImageJ Settings for Assessment based on Bankhead (2014) Instructions for Assessing Fluorescence in Z-stacks

1. Convert the CZI image file into a folder of TIFF image files using ZEN 2.5 (blue edition)'s image processing interface.
2. On ImageJ freeware, go to File -> Open -> locate and open all TIFF files of the folder created.
3. On ImageJ, open Image -> Stacks -> Images to Stacks. Title the name after the original data to keep information clear.
4. On ImageJ, open Image -> Stacks -> Z Project… It is going to automatically be set to Max Intensity, so hit Okay. ROS in image is set at Max Intensity now.
5. Saved the Max Intensity image in its dosage folder. The previous image without Max Intensity is deleted.
6. For analyzing ROS in *C. elegans*, we are looking at two distinct structures in the pharyngeal bulb. Referencing the ZEN pro images may be helpful in identifying the parts.
7. You will be taking three measurements: first bulb (metacorpus), second bulb (terminal bulb), and the overall pharyngeal pump (buccal cavity to end of terminal bulb). The bulbs are rough circles along the pharyngeal pump and used for food processing and a heartbeat equivalent.

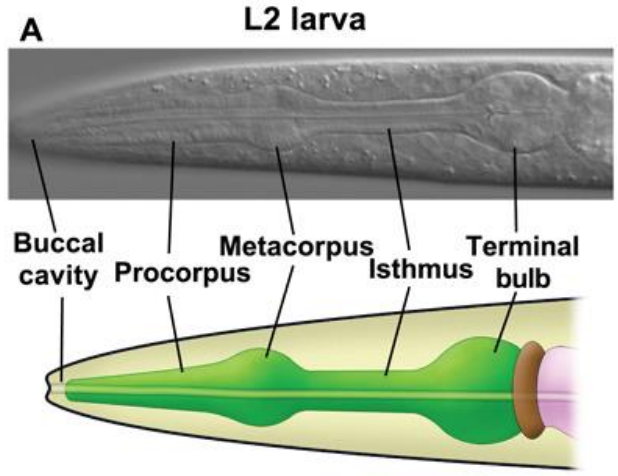

8. You will need to remove the background lighting of the image to stabilize any difference of the microscope. To do this, go to ImageJ's Process -> Subtract Background…
9. Specify 100 pixels and check Disable smoothing.
10. With the background removed, set measurements you will be taking by going to ImageJ's Analyze -> Set Measurements. Set to record min and max gray values, mean gray value, median, and display label.
11. Use the polygon selection on the toolbar to pinpoint measurements and record measurements.

12. For the overall pharyngeal bulb, measure from the point of the terminal bulb and go to the buccal tip. Try to keep the measurement lines within the body wall of the worm to remove background influence on the measurements.
13. Once those three measurements have been taken, record the mean, max, and median for each section.
14. Record measurements from every clear image taken of worms.

Appendix F: Zhang Lab Procedure for RNA Extraction, RT-PCR, and qRT-PCR from BIO6000 Biochemistry Course (Spring 2022)

RNA Extraction:

Three biological replicates of worms were collected from each treatment group and frozen at -80°C until ready for RNA extraction. Once ready, 400µL of Lysis/Binding buffer was added into each 2mL centrifuge tube containing the worms on ice. Sonicate each tube for 30 seconds using an Ultrasonic Converter on ice. Then add 40µL of miRNA Homogenate Additive to the tissue making sure to mix well either by vortexing or inverting tube several times before leaving the mixture on ice for 10 minutes. Then 400 µL of Acid-Phenol: Chloroform or matching that of previous miRNA homogenate was added into the lysate. Vortex for another 30 to 60 seconds, then centrifuge for 5 minutes at 10,000 x g at room temperature making sure to separate aqueous and organic phases. 300µL of aqueous phase was then collected and transferred into a fresh tube. Once transferred, 375 µL of 100% ethanol was added to the aqueous phase and mixed thoroughly by vortexing or inverting. For each sample, place a Filter Cartridge into a Collection Tube and pipet the lysate/ethanol mixture into a Filter Cartridge. Centrifuge for roughly 15 seconds at RCF 10,000 x g (10,000 rpm) to pass the mixture through the filter. Discard flow through and repeat until all lysate/ethanol mixture is through the filter. 700 µL of miRNA Wash Solution 1 was then added into the Filter Cartridge and centrifuged for 5 – 10 seconds to pull solution through the filter and then discard flow through again. A second wash of 500 µL of Wash Solution 2/3 was then used to wash through the filter again and centrifuged before discarding flow through. Finally, a third wash will then be repeated with Wash Solution 2/3. After discarding flow through and replacing the filter back into collection tube, centrifuge again for 1 minute to remove any residual liquid solutions from the sample before transferring to a new collection tube. Then apply 50 µL of pre-heated (95°C) nuclease-free water to the center of filter and close the cap and centrifuge for 30 seconds at max speed to recover RNA. If necessary, gently centrifuge again at low speed to make sure all collection sample is at the bottom of tube before measuring RNA concentration and quality using NanDrop-1000 based on the absorbance ratio of A260/280 and A260/230. Measurements below 1.8 for A260/280 and 2.0 for A260/230 were discarded due to contamination. Then RT-PCR was performed or store at -20°C or below until ready to be used.

RT-PCR via TaqMan® MicroRNA Reverse Transcription Kit:

Calculated volumes of 1µg of RNA sample and nuclease-free water needed per 15 µL RT reaction for each sample were made. Our 15 µL RT reaction included set amounts of RNase inhibitor (0.19 µL), 100 mM dNTPs (0.15 µL), 10X Reverse Transcription Buffer (1.50 µL), Multiscribe™ Reverse Transcriptase (1.00 µL), and primer mix (1.00 µL) along with calculated RNA sample and nuclease-free water. Once the reaction completed, the tubes were then gently mix and centrifuge to force the products to the bottom of tube (2000 rpm for 10 seconds) and then incubate tube on ice for 5 minutes and kept on ice until ready to load into thermal cycler. Once loaded in the thermal cycler, the process was as followed for RT-PCR: 30 minutes at 16°C, 30 minutes at 42°C, 5 minutes at 85°C, and will then hold at 4°C. After reverse transcription, 80 µL DNase free water will then be added into each RT-PCR product and then mixed before performing qRT-PCR or storing at -20°C or below until ready.

qRT-PCR:

Previous RT-PCR product will first need to be diluted with nuclease-free water before using. Using 96-well microplates, each well will be prepared by mixing in the following: 6 µL of nuclease-free water, 10 µL of SYBR Green PCR Master Mix, 2 µL of the RT-PCR (after diluting), and lastly 1 µL of forward and reverse primer specific to gene of interest. After loading each well of a 380-plate qRT-PCR plate, the microplate will then be sealed and centrifuged before loading for qRT-PCR using the 7300 Real-Time PCR System (Applied Biosystem). Run time of qRT-PCR is as the following: 10 minutes at 95°C for enzyme activation, 45 cycles of 15 second at 95°C to allow for denaturing along with 60 seconds at 60°C to allow for annealing. Once done, *tba-1* was used as the reference gene [18].

Appendix G: Summary Statistics of Reactive Oxygen Species

SAS summary statistics of each treatments' measured mean and median of the first bulb (metacorpus), second bulb (terminal bulb), and overall pharyngeal pump

Strain=N2

Treatment	N Obs	Variable	Label	Mean	Std Dev	Variance	Range	N	Lower 95% CL for Mean	Upper 95% CL for Mean
0	17	First_Bulb_Mean	First Bulb.Mean	91.8409412	30.6706975	940.6916851	103.2630000	17	76.0715236	107.6103587
		First_Bulb_Median	First.Bulb.Median	80.8235294	34.3988286	1183.28	113.0000000	17	63.1372837	98.5097751
		Second_Bulb_Mean	Second Bulb.Mean	113.7440588	39.5866870	1567.11	131.3140000	17	93.3904625	134.0976551
		Second_Bulb_Median	Second.Bulb.Median	111.0000000	42.2684871	1786.63	138.0000000	17	89.2675493	132.7324507
		Overall_Pump_Mean	Overall Pump.Mean	94.7792941	29.5982202	876.0546371	101.7800000	17	79.5612935	109.9972947
		Overall_Median	Overall.Median	89.0000000	31.1106895	967.8750000	108.0000000	17	73.0043595	104.9956405
14	8	First_Bulb_Mean	First Bulb.Mean	80.6771250	17.7842742	316.2804073	55.8150000	8	65.8090997	95.5451503
		First_Bulb_Median	First.Bulb.Median	81.5000000	18.8300671	354.5714286	60.0000000	8	65.7576699	97.2423301
		Second_Bulb_Mean	Second Bulb.Mean	110.7536250	18.0634429	326.2879688	54.7860000	8	95.6522088	125.8550412
		Second_Bulb_Median	Second.Bulb.Median	106.7500000	17.8785586	319.6428571	53.0000000	8	91.8031510	121.6968490
		Overall_Pump_Mean	Overall Pump.Mean	85.2178750	14.3738233	206.6067950	43.6740000	8	73.2010580	97.2346920
		Overall_Median	Overall.Median	80.8750000	16.4180867	269.5535714	54.0000000	8	67.1491360	94.6008640
140	13	First_Bulb_Mean	First Bulb.Mean	64.0474615	28.3401770	803.1656308	83.8440000	13	46.9216640	81.1732591
		First_Bulb_Median	First.Bulb.Median	57.6923077	29.5250871	871.7307692	90.0000000	13	39.8504761	75.5341393
		Second_Bulb_Mean	Second Bulb.Mean	84.0283077	41.2072161	1698.03	119.4110000	13	59.1270362	108.9295792
		Second_Bulb_Median	Second.Bulb.Median	76.3076923	43.1458469	1861.56	132.0000000	13	50.2349180	102.3804666
		Overall_Pump_Mean	Overall Pump.Mean	67.7645385	28.3873609	805.8422564	83.1220000	13	50.6102280	84.9188489
		Overall_Median	Overall.Median	59.5384615	28.7506968	826.6025641	89.0000000	13	42.1645894	76.9123337
700	8	First_Bulb_Mean	First Bulb.Mean	95.0148750	28.3138604	801.6746933	87.7380000	8	71.3438953	118.6858547
		First_Bulb_Median	First.Bulb.Median	94.5000000	34.1592907	1166.86	103.0000000	8	65.9421183	123.0578817
		Second_Bulb_Mean	Second Bulb.Mean	116.0741250	20.4723022	419.1151578	61.9970000	8	98.9588520	133.1893980
		Second_Bulb_Median	Second.Bulb.Median	113.2500000	26.2120474	687.0714286	85.0000000	8	91.3361800	135.1638200
		Overall_Pump_Mean	Overall Pump.Mean	96.8881250	24.2570629	588.4051027	73.6500000	8	76.6087129	117.1675371
		Overall_Median	Overall.Median	93.0000000	27.8772821	777.1428571	80.0000000	8	69.6940089	116.3059911

Appendix H. ANOVAs of Reactive Oxygen Species

Figure 1. ANOVA of metacorpus bulb, or "first bulb", of ROS treatments

Linear Models

The GLM Procedure
Least Squares Means
Adjustment for Multiple Comparisons: Tukey-Kramer

Strain=N2

Treatment	First_Bulb_Mean LSMEAN	LSMEAN Number
0	91.8409412	1
14	80.6771250	2
140	64.0474615	3
700	95.0148750	4

Least Squares Means for effect Treatment
Pr > |t| for H0: LSMean(i)=LSMean(j)

Dependent Variable: First_Bulb_Mean

i/j	1	2	3	4
1		0.7858	0.0459	0.9933
2	0.7858		0.5494	0.7326
3	0.0459	0.5494		0.0784
4	0.9933	0.7326	0.0784	

Figure 2. ANOVA of terminal bulb, or "second bulb" of ROS images

Linear Models

The GLM Procedure
Least Squares Means
Adjustment for Multiple Comparisons: Tukey-Kramer

Strain=N2

Treatment	Second_Bulb_Mean LSMEAN	LSMEAN Number
0	113.744059	1
14	110.753625	2
140	84.028308	3
700	116.074125	4

Least Squares Means for effect Treatment
Pr > |t| for H0: LSMean(i)=LSMean(j)

Dependent Variable: Second_Bulb_Mean

i/j	1	2	3	4
1		0.9971	0.1092	0.9986
2	0.9971		0.3302	0.9899
3	0.1092	0.3302		0.1853
4	0.9986	0.9899	0.1853	

Figure 3. ANOVA of overall pharyngeal pump of ROS images

Linear Models

The GLM Procedure
Least Squares Means
Adjustment for Multiple Comparisons: Tukey-Kramer

Strain=N2

Treatment	Overall_Pump_Mean LSMEAN	LSMEAN Number
0	94.7792941	1
14	85.2178750	2
140	67.7645385	3
700	96.8881250	4

Least Squares Means for effect Treatment
Pr > |t| for H0: LSMean(i)=LSMean(j)

Dependent Variable: Overall_Pump_Mean

i/j	1	2	3	4
1		0.8326	0.0391	0.9977
2	0.8326		0.4632	0.8129
3	0.0391	0.4632		0.0821
4	0.9977	0.8129	0.0821	

Appendix I. ANOVA results of significant genes of interest

Figure 1. ANOVA results of *eat-18* by treatment in genetic analysis

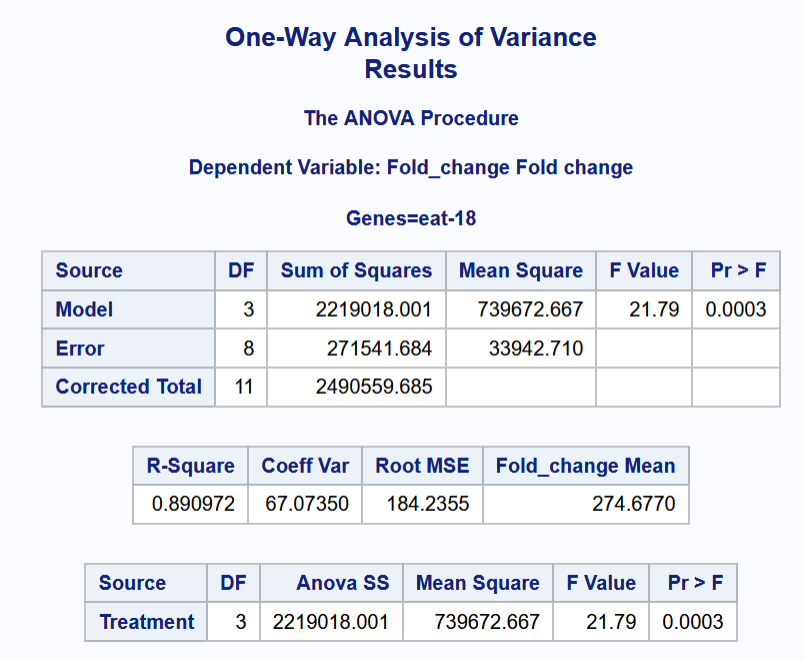

One-Way Analysis of Variance Results

The ANOVA Procedure

Dependent Variable: Fold_change Fold change

Genes=eat-18

Source	DF	Sum of Squares	Mean Square	F Value	Pr > F
Model	3	2219018.001	739672.667	21.79	0.0003
Error	8	271541.684	33942.710		
Corrected Total	11	2490559.685			

R-Square	Coeff Var	Root MSE	Fold_change Mean
0.890972	67.07350	184.2355	274.6770

Source	DF	Anova SS	Mean Square	F Value	Pr > F
Treatment	3	2219018.001	739672.667	21.79	0.0003

Figure 2. ANOVA analysis of *eat-18* significance between treatments and control in genetic analysis

Linear Models

The GLM Procedure
Least Squares Means
Adjustment for Multiple Comparisons: Tukey

Genes=eat-18

Treatment	Fold_change LSMEAN	LSMEAN Number
0.000	1.57033	1
14.000	8.37667	2
140.000	70.73000	3
700.000	1018.03100	4

Least Squares Means for effect Treatment
Pr > |t| for H0: LSMean(i)=LSMean(j)

Dependent Variable: Fold_change

i/j	1	2	3	4
1		1.0000	0.9658	0.0007
2	1.0000		0.9744	0.0007
3	0.9658	0.9744		0.0011
4	0.0007	0.0007	0.0011	

Treatment	Fold_change LSMEAN	95% Confidence Limits	
0.000	1.570333	-243.715640	246.856307
14.000	8.376667	-236.909307	253.662640
140.000	70.730000	-174.555974	316.015974
700.000	1018.031000	772.745026	1263.316974